LEVEL II

FAA-AM-79-4

PILOT PERFORMANCE DURING SIMULATED APPROACHES AND LANDINGS MADE WITH VARIOUS COMPUTER-GENERATED VISUAL GLIDEPATH INDICATORS

Mark F. Lewis
Henry W. Mertens
FAA Civil Aeromedical Institute
P.O. Box 25082
Oklahoma City, Oklahoma 73125

DISCLAIMER NOTICE

THIS DOCUMENT IS BEST QUALITY PRACTICABLE. THE COPY FURNISHED TO DTIC CONTAINED A SIGNIFICANT NUMBER OF PAGES WHICH DO NOT REPRODUCE LEGIBLY.

NOTICE

Technical Report Documentation Page

1. Report No.	2. Government Accession No.	3. Recipient's Catalog No.
FAA-AM-79-4		

4. Title and Subtitle
PILOT PERFORMANCE DURING SIMULATED APPROACHES AND LANDINGS MADE WITH VARIOUS COMPUTER-GENERATED VISUAL GLIDEPATH INDICATORS

5. Report Date
~~SEPTEMBER 1978~~ Jan 79

6. Performing Organization Code

8. Performing Organization Report No.

7. Author(s)
Mark F. Lewis and Henry W. Mertens

9. Performing Organization Name and Address
FAA Civil Aeromedical Institute
P.O. Box 25082
Oklahoma City, Oklahoma 73125

10. Work Unit No. (TRAIS)

11. Contract or Grant No.

13. Type of Report and Period Covered

12. Sponsoring Agency Name and Address
Office of Aviation Medicine
Federal Aviation Administration
800 Independence Avenue, S.W.
Washington, D.C. 20591

14. Sponsoring Agency Code

15. Supplementary Notes
Work was performed under Tasks AM-D-73/78-PSY-38.

16. Abstract

Two simulator experiments were conducted to quantify the effectiveness, in terms of pilot performance, of four different visual glidepath indicator systems in the severely reduced nighttime visual environment often referred to as the "black hole." A Convair 580 aircraft simulator was used with a computer-generated-image visual system attached for visual simulation of the airport scene. In Experiment I, four groups of six pilots flew simulated night approaches both with and without simulated glidepath indicators. Each group used a different type of indicator, either the standard Red/White 2-bar or 3-bar VASI system, the Australian T-VASIS, or a British experimental system (PAPI); all were designed to define a 3° glidepath. All indicators greatly reduced deviations from the 3° glidepath reference. Performance was best with the T-VASIS and decreased with the 3-bar VASI, PAPI, and 2-bar VASI in that order, but differences between the T-VASIS, 3-bar VASI, and PAPI were not statistically significant. Approaches flown without the ground-based glidepath indicators tended to be low and were extremely variable in this simulation where only runway lighting provided vertical guidance information. Experiment II compared the T-VASIS and 2-bar VASI regarding observing behavior in three pilots who made approaches with both systems. Observing behavior, measured by the frequency with which pilots pressed a button on the control wheel to get a 1-s look at the indicator during approaches, was significantly higher with the T-VASIS and also increased as distance from runway threshold decreased. Differences in performance with different indicators were attributed to the rate of information change provided by a given system and to rate of observing the indicator during approaches.

17. Key Words	18. Distribution Statement
Simulation Approach and landing Visual aids	Document is available to the public through the National Technical Information Service, Springfield, Virginia 22161

19. Security Classif. (of this report)	20. Security Classif. (of this page)	21. No. of Pages	22. Price
Unclassified	Unclassified	56	

Form DOT F 1700.7 (8-72) Reproduction of completed page authorized

084050

PILOT PERFORMANCE DURING SIMULATED APPROACHES AND LANDINGS MADE WITH VARIOUS COMPUTER-GENERATED VISUAL GLIDEPATH INDICATORS

Introduction.

The role of visual cues used by pilots making visual approaches and landings is incompletely understood. Not only do we not know how pilots land an airplane when presented with the "stimulus-rich" environment of an airport in daylight on a sunny day, we are also unable to specify the minimum cues needed to make a safe landing during less than ideal lighting or weather conditions. However, the development and use of visual glidepath indicator systems located next to many primary runways have eased the pilot's task in guiding his aircraft to the runway in a safe manner. Nevertheless, even with these Visual Approach Slope Indicators (VASI) systems in use, too many accidents continue to occur, especially when the availability of visual cues is reduced by darkness and/or inclement weather. These systems include three currently in international use, the 2-bar and 3-bar (Red/White) VASIs which are standard in the United States, the Australian "T" Visual Approach System (T-VASIS), and one experimental system, the Precision Approach Path Indicator (PAPI), a system that is currently under test in Great Britain and the United States.

The studies described in this paper represent an attempt to quantify, in terms of pilot performance, the effectiveness of four different visual glidepath indicator systems under conditions in which the stimulus environment is severely reduced. Although previous experiments (2,4) have compared performance with the T-VASIS and 2-bar VASI, these four indicators have not been compared in the same study and, to our knowledge, quantitative data on approach performance with the 3-bar VASI and PAPI systems have not been published. The most recent studies of 3-bar VASI, T-VASIS, and PAPI systems have involved subjective pilot assessments rather than performance measures (5,6,12,13,14).

EXPERIMENT I

Method.

Subjects. Twenty-four pilots with instrument and/or multiengine ratings served as subjects. All subjects had at least 20/30 acuity at the distances of 30 and 40 inches as measured by a test developed at the Civil Aeromedical Institute. All subjects were examined for color vision deficiencies with the Farnsworth Lantern; no evidence of color vision defect was indicated.

The 24 subjects were randomly assigned to four groups of six. Their experience levels varied from 360 hours to 24,000 hours of flying time.

The total flying time for each subject in each of the four groups is shown in Table 1.

TABLE 1. Total Hours of Flying Experience of Experimental Subjects

GROUP			
2-bar VASI	3-bar VASI	T-VASIS	PAPI
360	550	480	650
2,400	3,000	580	1,350
10,500	6,600	950	9,000
11,000	10,000	7,500	10,000
11,500	12,500	10,400	10,500
21,500	24,000	16,000	14,000

Apparatus. The subjects flew simulated VFR approaches in a fixed-base Convair 580 aircraft simulator with an attached computer-generated-image visual system that has been described elsewhere (9). A 17-in multicolor cathode-ray-tube display was mounted in front of the left-hand seat at eye height. This display was controlled by a Digital Equipment Corporation PDP-11/45 computer equipped with a VB11 display controller and an AD01 analog/digital conversion system. The display simulated a dynamic nighttime visual scene synchronized with the maneuvers of the aircraft simulator. Approaches were made to a simulation of Will Rogers World Airport (Oklahoma City), modified to align the main runways with magnetic north. The runway used for all approaches in this study was 9,800 ft in length, 170 ft wide (simulated separation between edge lights), and equipped with centerline and touchdown zone lighting. Lights simulated taxiways, terminal areas, and two other runways, but approach lighting was omitted. With these conditions the simulated scene represented what is usually described as a "black hole" environment, i.e.; the approach was made to an airport surrounded by darkness with no additional ground detail to aid the approach. Four types of ground-based visual glidepath indicator systems for vertical guidance were simulated. These included the standard 2-bar and 3-bar (red/white) VASI systems (16), the Australian "T" system (T-VASIS) (1), and a British experimental system (5) called the Precision Approach Path Indicator (PAPI). These visual glidepath indicators are described below. The intensity of all simulated lights varied with distance. The intensity of the lights in the scene was set in relation to runway lights to have a realistic appearance, with the exception of the

simulated red lights, which were relatively dimmer than in the natural situation due to limitations inherent in the penetration type of cathode-ray tube employed.

Procedure. At the beginning of each session, the subject's acuity and color vision were examined. The subject was acquainted with the simulator and the aims of the study. Recommended control settings, airspeeds, and vertical speeds for the maneuvers to be used in the experimental session were discussed when the subject was introduced to the simulator.

Since red lights were dimmer than in the natural situation, it was required that all subjects be able to see the red light bars in the glidepath systems at a simulated distance of at least 4 nautical miles from runway threshold as determined by a check during preexperimental familiarization with the simulator. The subjects were further instructed to adjust for the low relative intensity of red lights in the glidepath indicators by responding at far distances (greater than 4 miles) to the apparent absence of red lights. For example, with the 2-bar VASI, the "on glidepath" signal is red-over-white, the "high" signal is white-over-white, and the "low" signal is red-over-red. At far simulated distances (greater than 4 miles), subjects could identify these signals entirely in terms of the number of white bars visible, with two white bars indicating "high," one white bar indicating "on glidepath," and no light bars indicating "low." This strategy has been reported as being used by pilots in actual landings involving the PAPI system (14). However, in the present experiment performance was measured only at distances of 4 miles or less, a range within which the pilots were able to see all simulated lights and identify their color.

After at least two preliminary flights for practice, each subject flew six experimental missions consisting of takeoff, climb to 2,500 ft altitude, turn to heading of 180°, flight until approximately 8 miles south of the runway, turn to heading of 360° (approach heading), approach, and landing. The pilots were instructed to begin the approaches as soon as they had the runway in sight after turning to a heading of 360°. Basic flight instruments were always available including altimeter, vertical speed, airspeed, turn and bank, heading, and attitude indicators. All approaches, with or without glidepath indicators, were flown VFR, and in no case was ILS information available. A 10-minute break was given after the first three experimental flights. Each flight took approximately 10 minutes. The entire experimental session did not exceed 2 hours.

Each subject made three approaches with one type of glidepath indicator system and three approaches with no glidepath indicator. On approaches made with glidepath indicators, subjects were instructed to fly the glidepath defined by the indicator with as little deviation from that glidepath as possible. In all cases, glidepath indicators were designed to define 3° glidepaths. On approaches made without glidepath indicators, subjects were instructed to maintain a 3° glidepath as closely as possible. Order of glidepath-indicator and no-glidepath-indicator approaches were counterbalanced over subjects in each group. On all missions, east-west travel of the simu-

lator was fixed so that the task represented maneuvering in altitude and heading only. Once he had achieved the proper heading, the pilot could concentrate his attention on the glide slope.

Glidepath Indicator Systems.

2-bar VASI. A standard 2-bar VASI (16) was simulated with light bars on the left side of the runway. Both first (downwind) and second (upwind) light bars were 32 ft long and 50 ft to the left of the runway and were 650 and 1,350 ft respectively from the runway threshold. Each light bar appeared red when viewed from an angle less than the cutoff angle and white when viewed from a greater angle. Cutoff angles and light bar locations are presented in Figure 1. The appearance of the VASI lights when viewed from various vertical positions relative to the VASI glidepath is illustrated in Figure 2. When on the proper glidepath, the upwind bar appeared red and the downwind bar

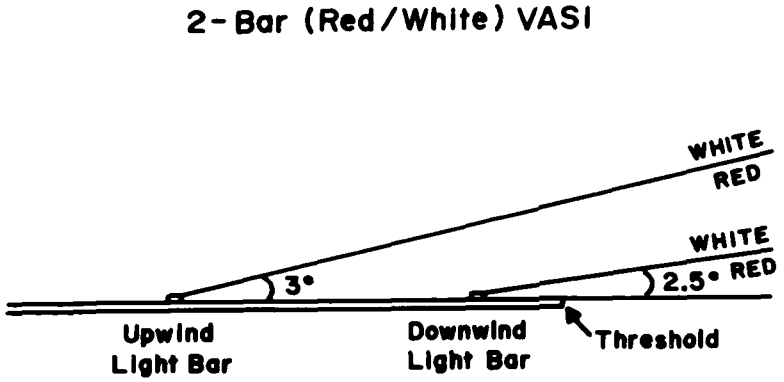

Figure 1. Cutoff angles of simulated light bars in the 2-bar VASI.

appeared white. Both bars appeared white when the approach was high and both appeared red when the approach was low. In actual VASI installations, the transition between red and white occurs gradually over a vertical angle of approximately one-fourth of a degree with the color changing from red to pink to white or vice versa. The actual apparent width of the pink zone is known to vary with ambient illumination and atmospheric conditions. Color transition in the present experiment represented the limiting case of instantaneous change as the cutoff angle was passed. All simulated red/white bars had this characteristic in this experiment. The implications of this difference between actual and simulated red/white light bars is considered in the discussion section of this paper.

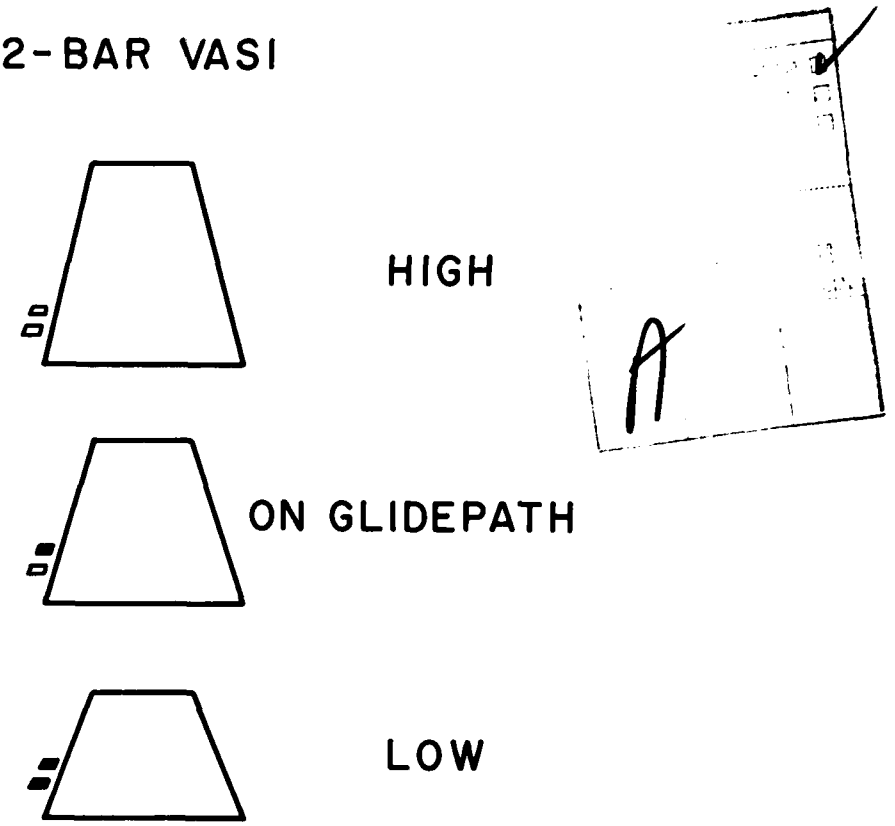

Figure 2. Illustration of 2-bar VASI signals. Open and closed rhomboids indicate white and red lights respectively.

3-bar VASI. A third bar was added to the standard 2-bar VASI 700 ft upwind of the second light bar of the 2-bar VASI configuration to produce a 3-bar VASI of the type used at airports handling large-bodied jet transports (16). The 3-bar VASI defines two glidepath zones (Figures 3 and 4). In the present experiment only the downwind zone as defined by the downwind and middle light bars was employed. Since the aiming angle of the middle light bar (which defined the upper limit of the glidepath) was 3°, the "effective glidepath angle" (as the term is used in Reference 16) was the same for both 2-bar and 3-bar VASIs, but the width of the visually defined glidepath was approximately twice as great in the case of the 2-bar VASI due to the difference in cutoff angles of the first light bar in the two systems.

T-VASIS. The Australian "T" Visual Approach System provides vertical guidance based on pattern of lights rather than color. Vertical guidance information is provided in terms of seven distinct zones of position relative to the ideal approach path (1). The T-VASIS consists of two parts, the "wing bar," which is always visible, and the position lights, which are not. The wing bar in the present experiment comprised two light bars 20 ft long separated laterally by 40 ft. The wing bar was centered on a point 50 ft to

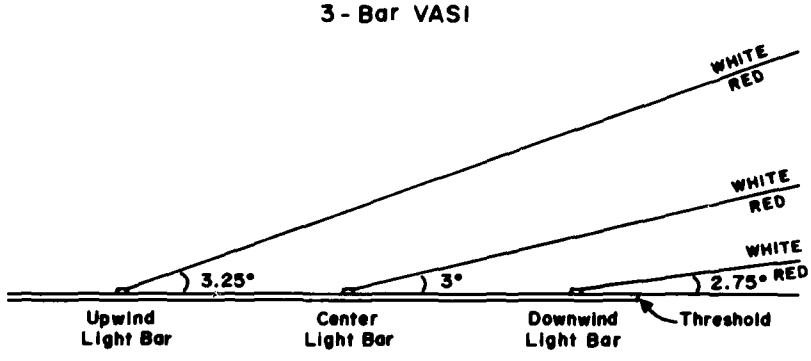

Figure 3. Cutoff angles of the simulated light bars in the 3-bar VASI.

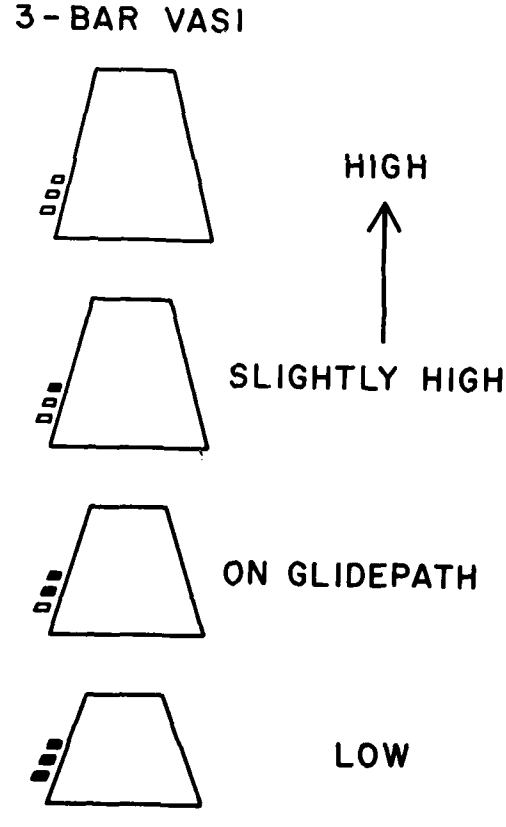

Figure 4. Illustration of 3-bar VASI signals. Open and closed rhomboids indicate white and red lights, respectively.

the left of the runway, 1,000 ft from threshold. The position lights consisted of six shorter light bars arrayed at equal 296-ft intervals on a line running parallel to the runway with three located upwind and three located downwind from the wing bar as shown in Figure 5 along with their respective cutoff angles.

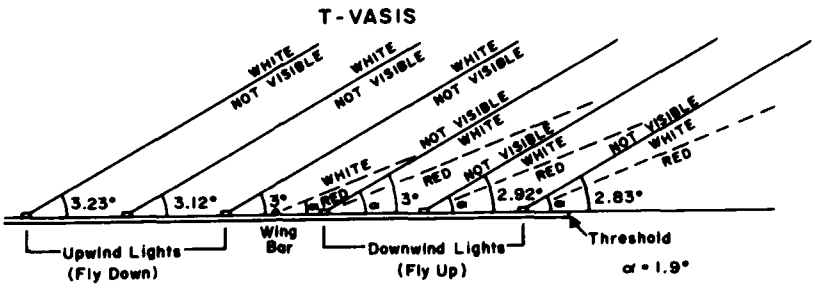

Figure 5. Cutoff angles of the simulated light units in the T-VASIS.

The three downwind units can be seen only when the aircraft's position is below the optimum glidepath. As illustrated in Figure 6, the number of downwind lights visible below the horizontal wing bar increases with deviation below the ideal path so that a "T" is formed whose vertical segment varies with deviations below the glidepath. Similarly, the number of upwind position lights visible increases with deviation above the optimum glidepath to form an inverted "T." When the aircraft deviates below a 1.9° glide slope, the transverse wing bar and all three downwind position lights in the "T" turn red. At approach angles less than 1.9°, all these units appear red. The "T" was set to define a 3° approach angle in the present experiment. Light boxes designed for the T-VASIS have a transition zone of 0.1° (in transition from visible to not visible). In the present experiment this transition was instantaneous as the cutoff angles were traversed.

PAPI. The British PAPI system (5) is an experimental system involving red/white light boxes that have a sharp red/white transition zone of 0.033° or less. It should be noted that this sharp transition of color was closely approximated by the present simulation. The PAPI system has four light units arrayed in each of two bars, one at 650 ft and one at 1,350 ft from threshold. The aiming angles of the light units in each bar are varied in small steps. In the downwind bar the innermost unit is set at an angle that is 0.08° below the glide slope angle; other light units in the same bar are set to progressively lower angles in 0.33° steps. The outermost light unit of the upwind bar is set at 0.08° above the optimum glidepath angle; other units of that bar have aiming angles which increase in 0.33° increments (Figure 7).

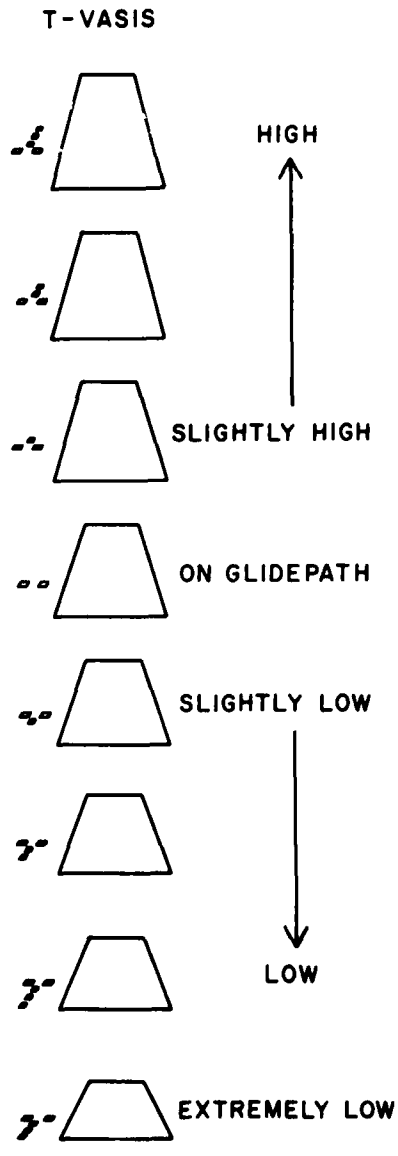

Figure 6. Illustration of T-VASIS signals. Open and closed rhomboids indicate white and red lights, respectively.

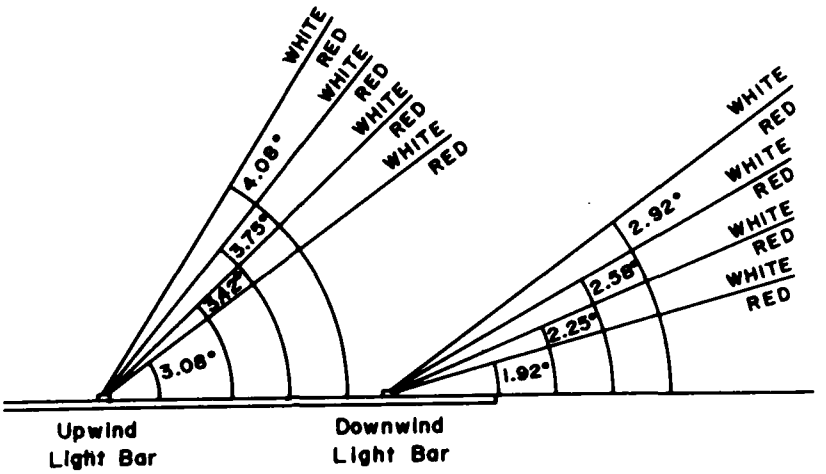

Figure 7. Cutoff angles of the simulated light units of the PAPI.

The simulated width and separation of light units in both bars was 10 ft. The normal red-over-white VASI signal is seen when on glidepath. As illustrated in Figure 8, as the aircraft starts to deviate below glide slope, one white light in the downwind bar will appear to turn red; with further descent below glidepath more light units in the downwind bar will turn red until all are red at an approach angle of 1.9°.

Increasing deviation above the optimum glidepath causes a similar gradual change of lights in the upwind bar from all red to all white. At a glidepath angle of 4.1° all light units appear white. Both T-VASI and PAPI provide greater information concerning both position with respect to the optimum approach path and the rate of closure of vertical deviation from the optimum path than do the 2-bar and 3-bar VASI systems. The T-VASIS is more sensitive to deviations than is the PAPI system.

Results.

The six subjects in each of the four glidepath indicator groups had three test trials, following practice, in which the glidepath indicator was used for vertical guidance during the approach and three test trials in which no glidepath indicator was used for vertical guidance. Simulated altitude and distance of the aircraft were recorded at 1-second intervals during all approaches. One aspect of the pilot's task in flying an approach is to produce or generate a glidepath that is as close as possible to an ideal approach path, commonly 3°, that intersects the runway plane 1,000 ft upwind from threshold. In the present experiment, the flight path profile (the function relating generated altitude to distance from threshold on the approach) was examined with regard to altitude deviations from the 3° path as a function of distance. Since the importance of a given altitude deviation

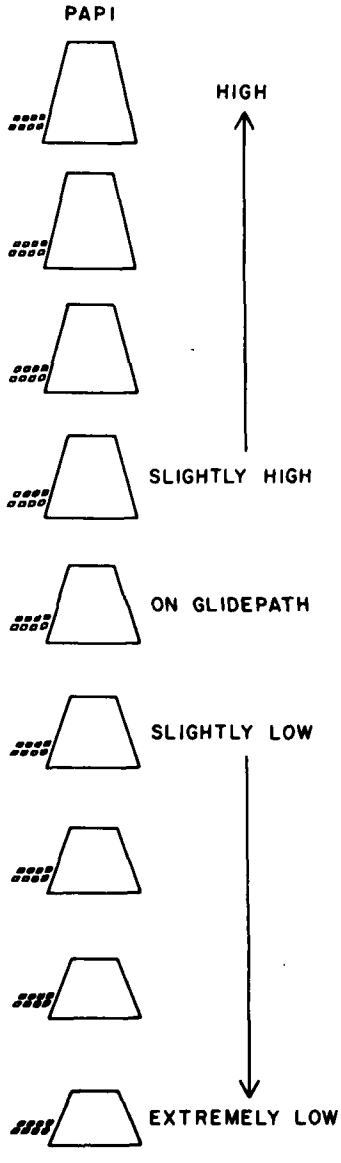

Figure 8. Illustration of PAPI signals. Open and closed rhomboids indicate white and red lights, respectively.

varies with distance from the aim point (1,000 ft upwind of threshold), a second analysis involved the magnitude of deviation from the 3° approach path in terms of generated approach angle (measured with respect to the ideal touchdown point) at each second during the approach. Generated approach angles were calculated by finding the angle whose tangent was the ratio of generated altitude to distance. Data for approaches made with glidepath indicators were analyzed separately from data obtained on trials with no glidepath indicator. The former are presented first.

Root mean square (RMS) altitude deviations, measured in feet, from the 3° approach path, as a function of indicator type, trials, and distance, were evaluated by analysis of variance. RMS altitude deviations were obtained for each of the four 1-nautical-mile segments of approaches for a distance of 24,000 ft to threshold. The only significant effects present in these data were the main effect of distance ($p < 0.01$) and the interaction of indicator type with trials ($p < 0.01$). Figure 9 shows the main effect of distance on RMS altitude deviations from the 3° approach path for each indicator type in each of the four 1-mile segments of approaches. The significant decrease in

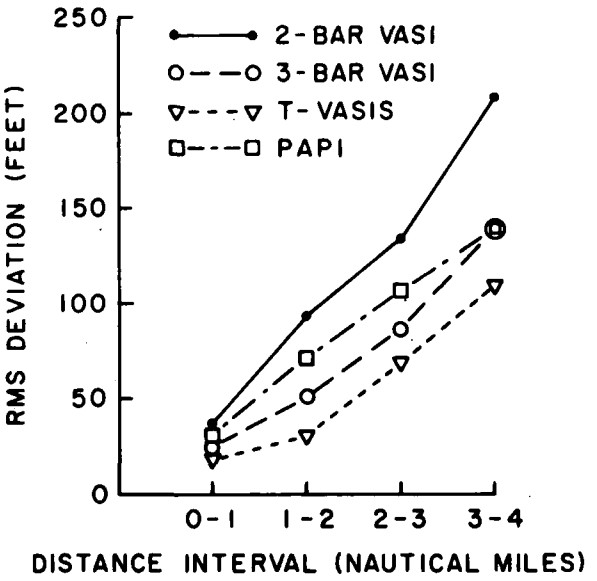

Figure 9. RMS altitude deviations as a function of glidepath indicator type and distance.

RMS deviations with distance is clear. The interaction of indicator type with trials is shown in Figure 10. No significant change in performance occurred over the three trials flown with the glidepath indicators except in the 2-bar

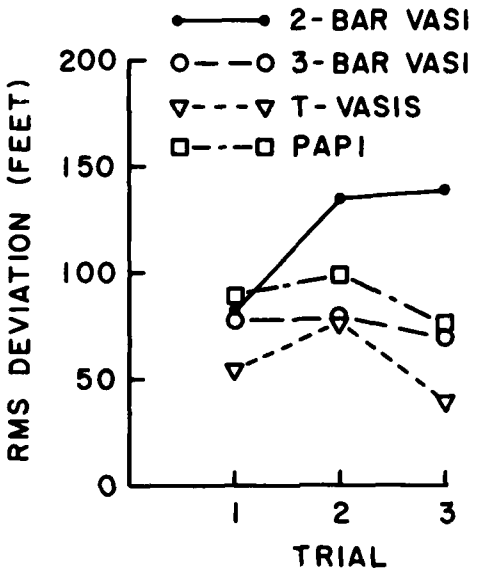

Figure 10. RMS altitude deviations as a function of glidepath indicator type and trials.

VASI group where deviations increased after the first trial. Analysis of individual cell means for this interaction showed that the only significant difference due to indicator type occurred on trial 3 between the 2-bar VASI and T-VASIS groups.

RMS generated approach angle deviations from 3^{o} were also analyzed as a function of indicator type, trials, and distance. Again, the only significant effects were the main effect of distance ($p < 0.01$) and the interaction of indicator type with trials ($p < 0.01$). RMS approach angle deviations are plotted as a function of indicator type and distance in Figure 11.

This illustration shows that the generated approach angle deviations are fairly constant until a distance from threshold of 1 nautical mile (2 miles in the case of the VASI group) at which point altitude deviations increase relative to distance by a statistically significant amount. The interaction of indicator type and trials is shown in Figure 12.

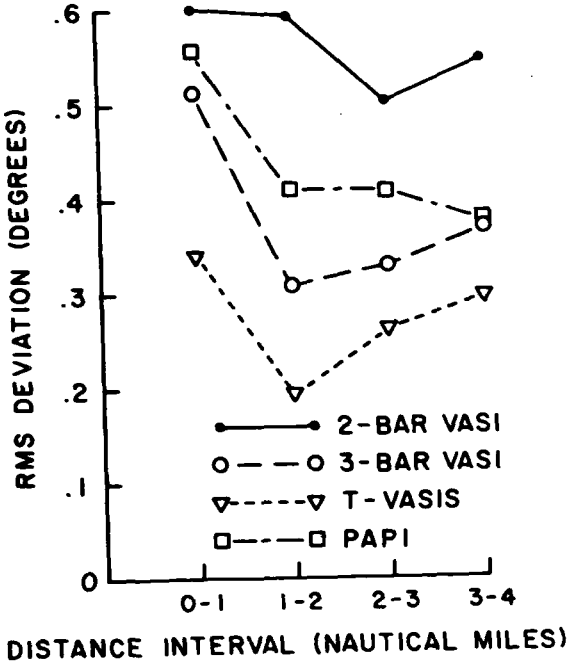

Figure 11. RMS generated approach angle deviations as a function of glidepath indicator type and distance.

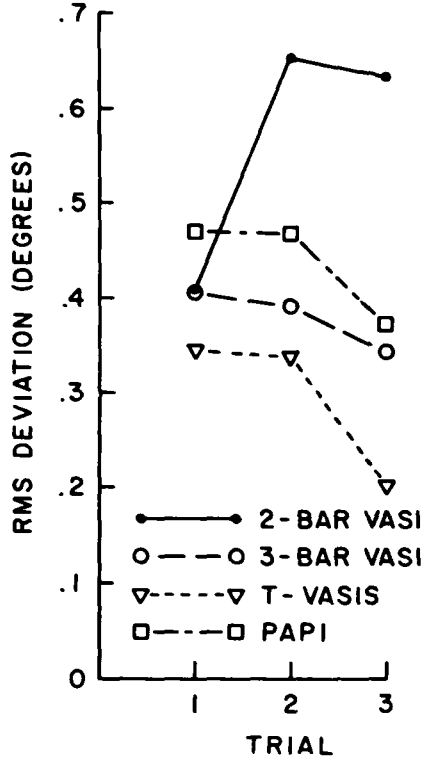

Figure 12. RMS generated approach angle deviations as a function of glidepath indicator type and trials.

RMS approach angle deviations in the 2-bar VASI group were significantly higher in trials 2 and 3 than in the 3-bar VASI and T-VASIS groups, and significantly higher than the PAPI group on trial 3. No differences among the three other groups were statistically significant.

Deviations in all four indicator groups were consistently much greater when visual indicators were not used in approaches. Only RMS generated approach angle deviations will be discussed, for brevity, concerning approaches made without glidepath indicators. There was a significant difference between indicator groups on approaches in the no-indicator trials. This can be seen in Figure 13 in which RMS generated approach angle deviations are

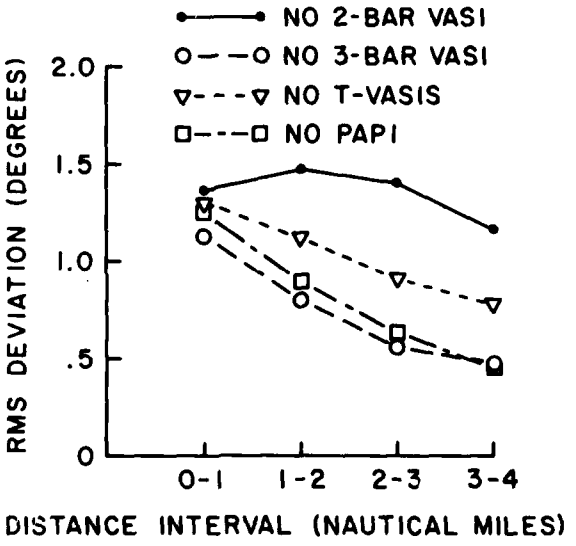

Figure 13. RMS generated approach angle deviations on no-indicator trials as a function of glidepath indicator type and distance.

plotted as a function of which indicator group subjects were in and distance interval. Analysis of simple effects revealed that on no-indicator trials the 2-bar VASI group had significantly higher RMS approach angle deviations than the 3-bar VASI and PAPI groups, but deviations of the 2-bar VASI group were not significantly greater than those of the T-VASIS group. On trials involving the glidepath indicator (shown in Figure 11), in contrast, the greatest difference occurred between the latter two groups. The significant ($p < 0.05$) interaction of indicator group and trials is shown in Figure 14. This effect reflects the fact that the significant difference between groups discussed above occurred only on trials 1 and 2 in the no-indicator condition.

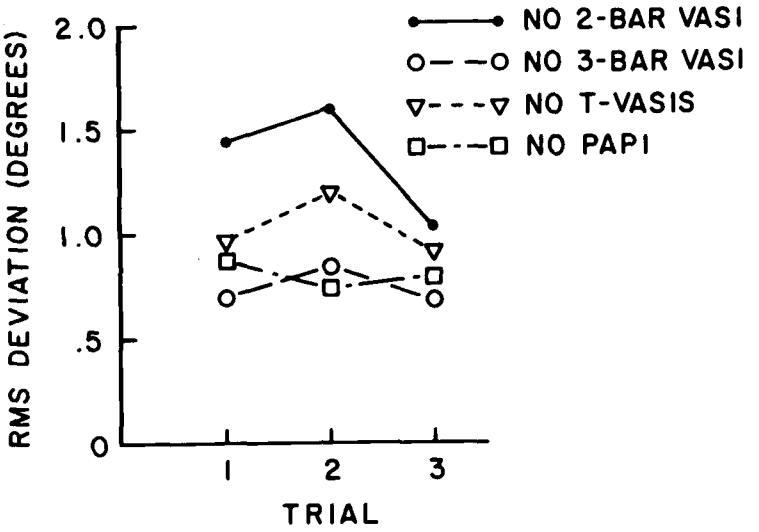

Figure 14. RMS generated approach angle deviations on no-indicator trials as a function of glidepath indicator type and trials.

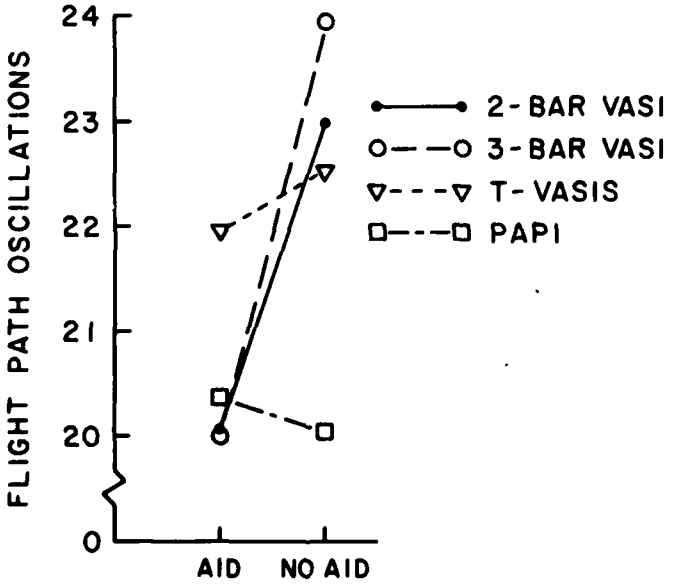

Figure 15. Flight path oscillations in indicator and no-indicator (no-aid) conditions as a function of glidepath indicator type.

The instability in approach paths flown with the different types of glidepath indicators was also studied. Flight path oscillations, a measure inversely related to stability, was measured in each of the approach flight profiles by counting peaks and troughs, or turning points, in the function relating altitude deviations (from the 3° path) to distance. The number of oscillations between the distances of 0 and 24,000 ft from threshold was calculated by dividing the sum of peaks and troughs in this distance range by 2. Oscillation data are summarized in Figure 15 for the four groups and approaches made with and without the glidepath indicators.

Only the 2-bar and 3-bar VASI systems produced a significant ($p < 0.01$) decrease in oscillations and there appears to be no correlation between number of oscillations and magnitude of deviations from the 3° glidepath.

Flight path profiles obtained in this experiment are summarized in terms of descriptive statistics for distributions of generated altitude at distance intervals of 1,000 ft over the range from runway threshold to 24,000 ft from threshold for each indicator type in Tables 2, 4, 6, and 8.

Similar descriptive statistics are given for the same groups under no-indicator conditions in Tables 3, 5, 7, and 9. The statistics presented for a particular distance and glidepath indicator condition are based on 18 observations (6 subjects x 3 trials) and include the high and low scores, the first (Q1), second (Q2, median), and third (Q3) quartiles, as well as the range, mean, standard deviation (unbiased estimate), and measures of skewness and kurtosis. Skewness and kurtosis measures were obtained using equations given by Kendall and Stuart (7). To facilitate interpretation of these data in terms of differences among groups regarding deviation from the 3° approach path and dispersion of generated altitudes in these distributions, generated altitude values in Tables 2, 4, 6, and 8 for highs, lows, and quartiles were converted to generated approach angles and plotted in Figures 16, 18, 20, and 22. Similar descriptive statistics are plotted for the no-glidepath indicator conditions for the four indicator types in Figures 17, 19, 21, and 23.

The descriptive statistics in these tables and figures indicate that flight paths tended to be lower and more variable when the glidepath indicators were not used. When glidepath indicators were used, the performance of groups in terms of both constant deviation errors measured with respect to the 3° approach path and variation of flight paths about that reference was ordered in terms of decreasing performance as follows: T-VASIS, 3-bar VASI, PAPI, and 2-bar VASI. Although overall performance with the 3-bar VASI was better than in two other groups, the only occurrence of short landings when using a glidepath indicator were with one subject in the 3-bar VASI group: On two occasions with the 3-bar VASI present, the subject landed short of runway threshold by as much as 450 ft. The only other short landing occurred during an approach with no visual glidepath indicator present with a subject in the PAPI group.

TABLE 2. 2-Bar VASI Group: Descriptive Statistics on 18 Approaches Made With the Indicator

DISTANCE (FT/1000)	Q1	Q2	Q3	HIGH	LOW	RANGE	MEAN	SD	SKEWNESS	KURTOSIS
0	43.4	51.5	62.1	79.5	14.4	65.1	51.3	14.4	-0.55780	3.92088
1	77.1	81.5	109.8	134.7	64.9	69.8	90.2	19.9	0.69128	2.40959
2	117.7	129.5	142.1	188.0	102.2	85.8	134.4	24.8	0.73115	2.74726
3	164.0	170.5	181.3	237.5	148.6	88.8	179.3	27.8	0.98112	2.64015
4	200.6	210.7	232.7	273.7	176.5	97.2	218.6	28.6	0.66302	2.37802
5	230.5	253.4	272.4	312.9	189.0	123.9	256.8	33.1	0.03391	2.47346
6	277.4	294.8	325.5	360.2	206.7	153.4	298.2	38.9	-0.26659	3.03753
7	311.2	334.0	377.1	407.5	222.5	185.0	339.0	46.7	-0.54828	3.28907
8	352.1	375.3	425.3	460.3	230.2	230.2	379.4	55.0	-0.87862	4.09914
9	390.2	431.5	459.6	514.3	230.0	284.4	421.2	67.5	-1.27481	4.83204
10	437.6	479.6	529.8	559.2	232.5	326.7	467.5	84.8	-1.46167	4.83119
11	479.3	530.8	595.4	639.4	244.6	394.7	516.8	103.6	-1.40472	4.51202
12	516.1	600.0	681.2	699.4	254.6	444.8	571.6	125.2	-1.30682	4.09841
13	580.5	663.2	713.8	774.4	254.6	519.8	618.8	142.3	-1.43795	4.32277
14	631.3	699.2	771.8	860.7	256.8	603.9	667.9	156.5	-1.49120	4.62932
15	671.7	766.7	814.0	947.4	287.4	659.9	721.5	169.9	-1.44959	4.56185
16	711.9	836.3	894.8	1041.9	328.8	713.1	777.0	184.8	1.39993	4.48409
17	780.9	881.7	941.8	1134.2	338.2	796.1	833.2	203.9	-1.37104	4.49549
18	851.0	921.5	1045.2	1229.2	347.8	881.4	891.1	223.2	-1.25422	4.26479
19	874.5	986.2	1096.2	1323.1	356.6	966.5	948.8	243.8	-1.10539	3.96419
20	878.8	1057.1	1183.5	1401.8	373.6	1028.2	1004.6	262.9	-1.00301	3.71465
21	911.2	1120.6	1253.0	1478.6	394.0	1084.6	1059.9	278.8	-0.88511	3.51459
22	960.1	1171.0	1311.0	1581.2	400.6	1180.6	1118.7	296.6	-0.79538	3.49612
23	1033.4	1195.6	1376.5	1681.8	420.3	1261.6	1181.2	313.5	-0.70666	3.50069
24	1099.6	1243.4	1430.1	1771.0	463.0	1308.0	1245.3	328.2	-0.58528	3.33530

TABLE 3. 2-Bar VASI Group: Descriptive Statistics on 18 Approaches Made Without the Indicator

DISTANCE (FT/1000)	Q1	Q2	Q3	HIGH	LOW	RANGE	MEAN	SD	SKEWNESS	KURTOSIS
0	34.1	56.0	106.6	138.1	15.5	122.7	68.7	41.3	0.58135	1.93888
1	62.1	90.0	135.1	215.4	27.6	187.8	107.1	58.9	0.71689	2.21351
2	87.4	132.7	163.0	297.9	62.5	235.4	149.1	74.8	0.77992	2.29764
3	124.5	164.5	203.9	374.8	68.8	306.0	184.2	91.6	0.77603	2.44880
4	125.2	188.8	241.2	457.7	55.3	402.3	213.9	112.8	0.78630	2.59843
5	147.3	212.7	290.3	553.1	30.3	522.8	242.6	138.3	0.74178	2.75571
6	167.8	245.1	334.5	643.7	12.6	631.1	271.4	165.6	0.71858	2.75681
7	168.7	249.8	365.0	734.1	27.3	706.8	302.2	191.1	0.82344	2.76507
8	175.0	259.4	409.7	822.1	63.6	758.4	336.8	216.8	0.91333	2.73271
9	187.0	281.9	453.3	893.3	95.7	797.7	374.2	239.0	0.90698	2.61606
10	192.7	307.0	504.0	953.3	122.3	831.0	406.0	259.2	0.88030	2.52632
11	204.7	327.4	541.9	1013.3	111.8	901.5	437.4	283.7	0.86545	2.45530
12	209.4	358.6	587.5	1082.5	109.9	972.5	471.5	310.7	0.83106	2.36930
13	242.9	394.1	654.2	1150.0	96.9	1053.0	510.3	334.4	0.75273	2.26726
14	289.1	438.6	714.7	1217.4	90.3	1127.1	553.1	352.7	0.70737	2.25281
15	334.9	469.6	779.9	1299.5	93.3	1206.1	597.3	370.1	0.67332	2.24316
16	371.4	507.1	844.6	1374.4	126.1	1248.3	642.3	384.2	0.66166	2.20234
17	382.6	552.5	916.7	1455.6	184.7	1270.9	687.2	398.3	0.66712	2.17315
18	413.3	589.5	994.7	1533.6	234.5	1299.1	733.0	413.1	0.66063	2.15179
19	483.4	617.7	1061.9	1600.7	283.6	1317.1	777.8	423.8	0.65578	2.13193
20	539.9	643.8	1127.2	1681.2	336.7	1344.5	826.2	433.6	0.64999	2.13870
21	587.5	697.4	1200.0	1751.6	392.4	1359.2	881.9	442.0	0.62146	2.12795
22	640.3	763.0	1285.8	1812.3	406.8	1405.5	940.8	452.5	0.55474	2.10242
23	692.2	830.0	1366.8	1878.7	424.1	1454.6	1001.2	463.1	0.56021	2.08676
24	712.3	895.0	1415.5	1947.0	443.6	1503.4	1059.9	472.8	0.53538	2.06243

TABLE 4. 3-Bar VASI Group: Descriptive Statistics on 18 Approaches Made With the Indicator

DISTANCE (FT/1000)	Q1	Q2	Q3	HIGH	LOW	RANGE	MEAN	SD	SKEWNESS	KURTOSIS
0	33.5	43.1	52.2	80.2	0.0	80.2	41.5	20.5	-0.36729	3.29041
1	77.8	92.1	107.2	137.8	28.9	108.9	88.1	27.3	-0.56316	3.18707
2	118.5	139.7	159.3	191.9	108.6	83.3	142.5	25.3	0.34864	2.09620
3	186.5	198.4	213.2	239.2	163.1	76.1	200.5	22.7	0.14191	2.14252
4	231.1	260.9	272.9	307.9	213.9	94.0	255.8	26.0	0.04971	2.14834
5	274.1	313.5	327.9	363.5	252.8	110.7	307.5	34.0	-0.13551	1.97926
6	318.1	362.0	394.8	422.0	305.6	116.4	360.7	40.0	-0.05354	1.62670
7	373.3	407.7	441.0	492.9	350.5	142.5	412.4	45.2	0.37235	1.93305
8	424.8	443.8	481.7	585.5	399.7	185.8	461.5	51.0	1.08922	3.24210
9	470.2	477.7	532.3	615.4	448.3	167.1	499.5	48.2	1.07141	2.96373
10	510.2	523.2	554.6	679.4	467.6	211.8	537.1	51.0	1.34409	4.57270
11	542.4	565.5	597.6	754.6	494.7	259.9	579.6	63.5	1.27161	4.58306
12	586.7	612.6	657.1	824.5	531.6	292.9	631.2	73.3	1.23767	4.20579
13	637.9	658.9	714.7	878.2	611.7	266.5	688.6	74.2	1.47599	4.42055
14	699.6	710.5	764.7	938.2	643.2	294.9	740.6	79.8	1.61211	4.67392
15	739.7	771.5	819.1	1010.1	668.9	341.2	791.4	92.2	1.23325	3.82905
16	792.3	832.9	876.1	1099.1	711.5	387.6	851.6	104.3	1.05613	3.39770
17	831.6	891.4	945.6	1178.1	750.9	427.2	913.9	120.5	0.97154	2.97047
18	878.5	944.4	1036.7	1242.8	793.0	449.9	976.9	134.2	0.84388	2.64959
19	935.4	1001.6	1134.7	1347.1	829.7	517.4	1037.9	149.5	0.72859	2.51024
20	980.7	1051.1	1240.7	1436.1	876.4	559.6	1098.1	161.6	0.70746	2.38451
21	1028.8	1112.6	1351.4	1519.6	934.7	584.9	1162.3	173.2	0.67379	2.20883
22	1086.5	1167.4	1442.9	1604.6	999.7	604.9	1225.8	186.6	0.65009	2.12305
23	1143.6	1225.4	1513.2	1687.0	1049.5	637.5	1293.1	198.7	0.63626	2.09957
24	1201.0	1277.6	1578.7	1768.9	1108.2	660.7	1361.6	209.0	0.66278	2.12084

TABLE 5. 3-Bar VASI Group: Descriptive Statistics on 18 Approaches Made Without the Indicator

DISTANCE (FT/1000)	Q1	Q2	Q3	HIGH	LOW	RANGE	MEAN	SD	SKEWNESS	KURTOSIS
0	30.4	39.9	71.8	203.4	13.3	190.1	54.3	44.0	2.26178	8.36300
1	60.2	90.6	132.6	248.6	26.1	222.5	99.2	54.4	1.06234	4.11608
2	75.5	129.8	194.1	305.2	55.9	249.3	143.5	69.9	0.59685	2.58701
3	110.3	168.0	250.7	354.1	74.7	279.3	186.7	83.2	0.35114	2.05180
4	162.7	214.0	314.1	413.7	96.2	317.6	233.1	93.8	0.25703	2.03474
5	211.9	274.5	347.7	470.2	123.9	346.4	281.7	104.5	0.11034	2.06428
6	257.8	326.3	399.8	519.7	151.4	368.4	328.9	115.1	0.16640	1.96175
7	278.0	347.8	465.6	578.1	188.7	389.4	373.5	125.7	0.29980	1.87646
8	302.7	398.0	524.7	657.1	247.5	409.7	423.2	137.4	0.41226	1.82196
9	342.1	432.9	581.2	725.6	241.7	483.9	475.5	149.1	0.39041	1.91651
10	408.2	468.9	653.6	797.7	268.7	529.0	526.4	157.3	0.35668	1.89852
11	450.0	531.3	718.3	875.5	347.6	527.9	584.8	164.9	0.42710	1.81868
12	507.8	605.1	777.7	946.2	389.5	556.7	643.1	169.6	0.36845	1.87605
13	578.9	670.0	847.6	1009.8	380.6	629.2	704.3	175.1	0.17777	2.11625
14	662.3	728.1	916.7	1073.4	380.3	693.2	763.0	182.2	-0.02479	2.50505
15	724.4	799.8	966.5	1134.7	383.4	751.3	824.3	190.4	-0.28601	2.95973
16	781.3	867.0	1016.8	1193.8	409.0	784.8	884.7	196.7	-0.42436	3.23176
17	858.0	946.8	1071.9	1264.8	419.1	845.7	947.8	204.4	-0.64288	3.78046
18	908.2	1022.3	1126.1	1334.7	431.5	903.2	1008.0	213.7	-0.88562	4.22805
19	963.6	1085.8	1187.2	1394.5	466.3	928.2	1068.1	218.9	-1.00581	4.41476
20	1025.6	1161.8	1253.3	1465.5	528.6	937.0	1131.6	222.6	-0.95316	4.22293
21	1092.8	1233.3	1326.0	1538.1	590.0	948.1	1197.5	227.2	-0.90759	4.05787
22	1159.3	1291.5	1409.2	1599.3	632.5	966.9	1262.7	233.6	-0.95393	4.11706
23	1218.4	1345.9	1495.7	1664.1	682.2	981.9	1327.2	240.9	-0.92530	4.02209
24	1283.4	1401.1	1581.5	1719.9	739.6	980.3	1392.0	244.5	-0.91787	3.96429

TABLE 6. T-VASIS Group: Descriptive Statistics on 18 Approaches Made With the Indicator

DISTANCE (FT/1000)	Q1	Q2	Q3	HIGH	LOW	RANGE	MEAN	SD	SKEWNESS	KURTOSIS
0	44.0	48.2	58.8	73.7	18.3	55.4	49.0	13.5	-0.12018	3.10342
1	88.5	97.1	101.1	139.9	76.2	63.7	99.5	17.3	0.97529	3.18149
2	148.2	150.5	162.1	202.0	132.9	69.1	157.0	17.5	1.16470	3.85094
3	196.5	208.8	219.1	269.0	183.8	85.2	212.1	22.0	1.01805	3.74182
4	246.9	260.0	268.5	326.1	229.6	96.5	263.4	25.2	1.14972	3.73262
5	299.8	310.8	318.0	373.9	271.8	102.0	315.7	26.1	1.01717	3.60685
6	349.0	359.4	375.3	439.2	328.5	110.8	368.8	29.8	1.01610	3.20972
7	398.3	406.6	419.1	502.6	376.1	126.4	416.2	33.3	1.40274	4.22841
8	435.5	456.1	475.8	538.9	419.8	119.1	461.5	35.4	0.91588	3.23533
9	479.8	505.9	530.1	598.4	452.5	145.9	507.9	35.5	0.76130	3.50341
10	532.8	551.9	572.2	661.6	504.2	157.4	556.8	34.8	1.39416	5.70510
11	579.5	590.9	628.0	702.7	555.7	147.1	606.4	37.5	1.03028	3.49257
12	622.2	653.5	682.3	742.5	576.8	165.7	654.8	43.6	0.27275	2.46732
13	664.8	707.8	718.0	898.5	606.1	292.3	703.9	61.2	1.68224	7.00427
14	708.4	758.9	779.5	1047.1	658.3	388.8	758.6	83.5	2.28968	9.13990
15	753.8	803.4	843.4	1148.8	705.3	443.5	810.7	96.3	2.42693	9.65247
16	798.5	840.3	882.1	1264.6	708.3	556.2	857.8	115.5	2.45790	9.84308
17	844.4	886.1	927.2	1378.8	754.0	624.9	910.4	131.7	2.58385	10.16557
18	885.8	922.6	999.9	1462.0	812.2	649.8	965.9	140.9	2.53485	9.74814
19	934.6	976.7	1045.3	1550.2	876.2	673.9	1023.1	151.5	2.46781	9.28555
20	985.0	1040.6	1105.7	1640.9	943.8	697.1	1080.4	161.6	2.44945	9.16339
21	1039.4	1095.1	1169.7	1709.1	990.6	718.5	1133.9	166.0	2.43602	9.13408
22	1097.9	1145.7	1232.8	1739.8	1026.6	713.2	1188.9	161.7	2.29234	8.58161
23	1156.0	1191.3	1312.3	1834.7	1077.8	757.0	1250.2	169.9	2.35494	8.91246
24	1212.8	1266.4	1373.2	1903.5	1139.8	763.7	1314.4	174.0	2.23013	8.37400

TABLE 7. T-VASIS Group: Descriptive Statistics on 18 Approaches Made Without the Indicator

DISTANCE (FT/1000)	Q1	Q2	Q3	HIGH	LOW	RANGE	MEAN	SD	SKEWNESS	KURTOSIS
0	40.8	47.8	85.4	229.8	12.6	217.2	64.6	47.8	2.40795	9.06627
1	67.5	92.8	125.0	280.7	41.7	239.1	101.3	57.9	1.77276	6.08561
2	102.3	132.3	201.2	362.3	55.8	306.5	145.8	78.2	1.17514	4.27642
3	119.4	164.3	273.7	505.0	51.2	453.8	192.7	108.4	1.29997	4.84745
4	142.3	199.8	332.1	636.9	66.5	570.5	238.1	135.3	1.42537	5.14583
5	164.2	235.9	388.2	716.4	104.6	611.8	282.3	153.3	1.25963	4.46088
6	195.2	280.2	458.7	799.9	116.5	683.4	327.5	175.1	1.06466	3.84840
7	226.3	329.4	540.6	897.0	124.1	772.9	377.4	199.8	0.94474	3.48884
8	242.3	395.7	621.2	977.2	146.2	831.0	431.9	217.9	0.80556	3.14799
9	289.9	454.1	704.3	1055.6	148.4	907.2	487.3	232.6	0.69821	2.99589
10	330.7	513.1	767.2	1127.0	173.3	953.8	543.4	246.2	0.57843	2.81819
11	373.3	572.6	827.4	1196.3	220.2	976.1	601.7	259.2	0.47601	2.61205
12	425.1	649.9	898.5	1267.3	281.5	985.8	662.4	271.8	0.40639	2.44687
13	462.2	726.5	974.6	1330.8	332.4	998.4	722.7	283.0	0.32828	2.31043
14	490.2	803.0	1044.2	1403.3	344.0	1059.3	786.0	296.6	0.22377	2.21933
15	529.0	867.0	1102.9	1454.8	344.8	1110.0	847.7	308.1	0.11366	2.10935
16	595.2	930.2	1174.0	1508.8	365.6	1143.2	910.9	317.0	0.04527	2.05459
17	685.2	994.7	1245.2	1573.1	420.7	1152.4	976.3	321.5	0.02975	2.02536
18	760.8	1065.6	1321.8	1650.7	480.5	1170.2	1045.4	329.8	0.01278	2.02072
19	828.7	1131.5	1409.3	1712.9	564.1	1148.8	1112.0	340.9	-0.01323	1.94421
20	897.1	1186.7	1477.8	1735.3	587.5	1147.8	1176.8	344.1	-0.07209	1.88571
21	969.4	1234.8	1541.0	1812.8	607.4	1205.4	1243.1	350.5	-0.07054	1.95368
22	1038.4	1300.7	1607.5	1868.1	623.4	1244.8	1306.7	350.7	-0.12596	2.05045
23	1108.3	1373.5	1686.0	1921.9	633.3	1288.5	1371.0	352.2	-0.21159	2.24067
24	1172.2	1439.8	1754.2	1995.5	650.9	1344.6	1435.2	355.7	-0.27755	2.44458

TABLE 8. PAPI Group: Descriptive Statistics on 18 Approaches Made With the Indicator

DISTANCE (FT/1000)	Q1	Q2	Q3	HIGH	LOW	RANGE	MEAN	SD	SKEWNESS	KURTOSIS
0	43.8	59.4	66.7	142.4	35.1	107.4	62.6	26.3	1.77696	6.06093
1	86.7	110.1	129.8	167.2	71.9	95.3	110.7	27.6	0.57562	2.43430
2	136.3	155.5	170.2	223.5	114.0	109.5	158.1	29.7	0.83033	3.16157
3	177.0	192.5	218.4	301.5	161.1	140.4	204.9	40.0	1.46456	4.43100
4	230.1	241.0	269.5	375.6	191.9	183.7	254.1	47.4	1.37531	4.45303
5	274.2	294.8	319.6	409.9	232.9	177.1	302.0	47.2	0.77224	3.34456
6	311.3	355.2	374.4	426.4	272.9	153.5	348.1	42.2	-0.10477	2.23701
7	351.0	400.8	435.1	454.9	329.0	125.9	394.3	44.6	-0.18107	1.58890
8	395.4	436.7	484.5	562.7	339.9	222.9	437.5	58.6	0.32334	2.42739
9	438.2	464.1	525.3	660.8	357.7	303.0	482.4	74.7	0.58246	3.08721
10	490.4	495.5	576.8	708.6	383.8	324.8	527.0	84.1	0.42413	2.75262
11	522.8	554.2	654.3	775.1	396.9	378.2	571.3	97.9	0.36042	2.62795
12	555.1	587.7	704.9	815.6	399.8	415.9	608.6	104.1	0.08303	2.59769
13	594.4	644.6	746.4	846.7	429.4	417.3	654.8	106.9	-0.12402	2.46771
14	651.4	700.2	794.8	850.5	479.8	370.7	706.7	106.3	-0.35189	2.33238
15	706.0	751.4	846.2	924.9	513.3	411.6	759.3	111.3	-0.54220	2.69243
16	730.0	812.1	889.1	996.1	540.7	455.4	807.6	120.4	-0.47098	2.82342
17	794.8	862.4	941.2	1056.1	584.2	471.9	860.1	123.6	-0.47055	2.99952
18	831.0	931.8	995.7	1146.8	654.4	492.5	914.2	132.1	-0.15815	2.61601
19	881.0	978.9	1056.1	1234.5	705.0	529.6	965.2	143.5	-0.12142	2.60259
20	934.8	1031.7	1103.5	1328.0	723.5	604.5	1015.6	155.1	-0.12506	2.81265
21	998.5	1072.7	1163.5	1416.6	795.3	621.2	1072.7	162.6	-0.02750	2.83489
22	1070.2	1120.7	1260.9	1492.7	831.3	661.5	1131.5	176.6	-0.12956	2.71739
23	1134.3	1188.9	1350.9	1563.2	832.3	730.9	1194.5	193.6	-0.26967	2.56277
24	1197.4	1250.1	1438.9	1625.6	833.3	792.3	1259.8	210.1	-0.41344	2.52869

TABLE 9. PAPI Group: Descriptive Statistics on 18 Approaches Made Without the Indicator

DISTANCE (FT/1000)	Q1	Q2	Q3	HIGH	LOW	RANGE	MEAN	SD	SKEWNESS	KURTOSIS
THRESHOLD	15.5	36.0	59.8	159.1	0.0	159.1	49.3	45.6	1.16562	3.30976
1	48.9	70.1	97.4	208.4	28.1	180.2	87.6	53.9	1.03101	2.91035
2	84.4	109.4	140.4	251.3	65.8	185.5	128.9	61.4	1.02817	2.62658
3	110.6	154.9	183.2	305.2	85.4	219.8	168.5	70.3	0.87939	2.50954
4	140.2	197.9	226.9	365.9	101.9	264.0	203.7	80.3	0.74789	2.53687
5	164.0	233.1	271.9	414.6	133.4	281.2	241.1	88.4	0.76434	2.59172
6	208.3	260.7	320.2	474.3	159.6	314.7	278.6	99.2	0.64259	2.37129
7	232.2	301.7	375.1	548.2	180.0	368.2	320.5	112.8	0.56343	2.27065
8	261.8	342.4	443.7	625.6	207.8	417.8	365.2	127.6	0.54349	2.21791
9	281.5	390.6	520.1	696.6	224.6	472.0	409.9	144.1	0.49240	2.12146
10	322.4	436.8	602.6	713.4	238.1	475.3	457.3	152.5	0.27361	1.84674
11	374.6	493.9	651.7	785.2	259.6	525.6	512.5	162.9	0.19805	1.87405
12	450.0	552.4	705.2	842.3	283.5	558.8	568.4	167.5	0.08385	1.95245
13	519.6	614.3	715.9	905.5	303.1	602.4	624.4	175.0	-0.00389	2.14697
14	571.9	682.3	787.5	959.6	330.7	628.9	681.9	181.6	-0.07399	2.34383
15	629.8	741.0	836.3	1020.7	373.5	647.2	744.5	186.3	-0.09361	2.49381
16	700.4	799.0	905.9	1104.1	434.9	669.2	807.2	190.5	0.01476	2.41844
17	762.3	863.5	976.3	1179.1	495.3	683.8	876.4	188.9	0.00034	2.46129
18	822.1	929.0	1039.3	1252.5	561.8	690.7	943.3	188.3	-0.00691	2.42134
19	883.7	977.6	1122.5	1336.1	645.4	692.7	1009.3	191.8	0.07750	2.24890
20	947.7	1023.1	1205.3	1412.7	713.7	699.0	1070.9	197.4	0.13368	2.10879
21	997.3	1068.7	1270.3	1478.6	790.8	687.8	1129.6	201.7	0.21249	1.94820
22	1041.1	1125.8	1323.0	1546.5	882.8	663.8	1194.5	203.1	0.28173	1.87587
23	1092.5	1193.9	1393.9	1601.9	969.0	633.0	1260.2	202.0	0.28393	1.84439
24	1145.2	1270.7	1463.0	1657.4	1038.7	618.7	1325.2	202.5	0.25142	1.82386

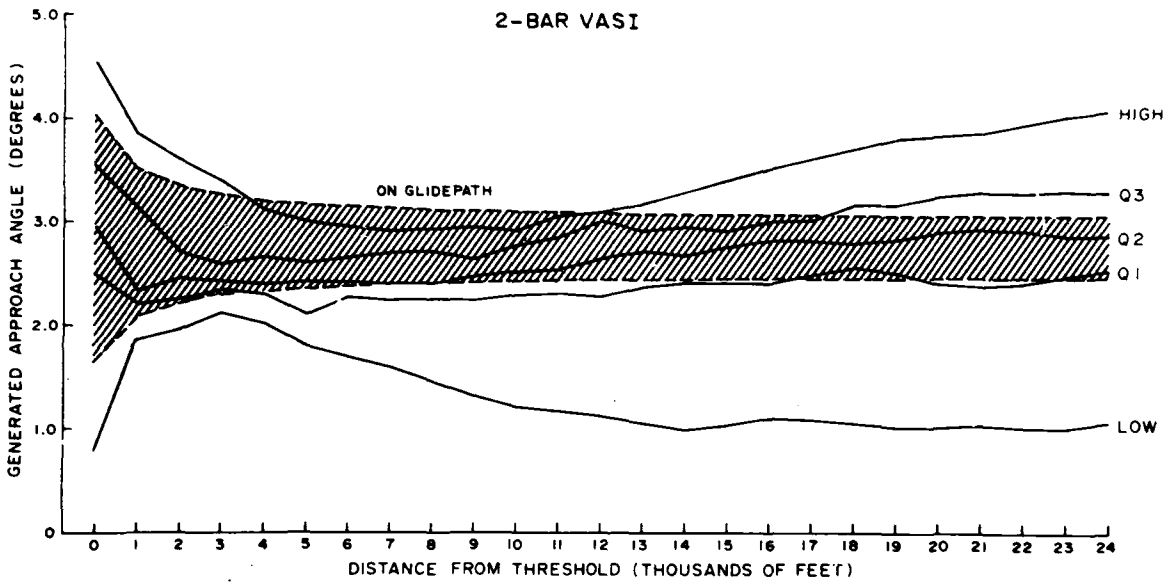

Figure 16. High scores, low scores, and quartiles of generated approach angle distributions at 1,000-ft distance intervals on approaches in which the 2-bar VASI was utilized. The range of generated approach angles that would be within the glidepath is indicated by the hatched area.

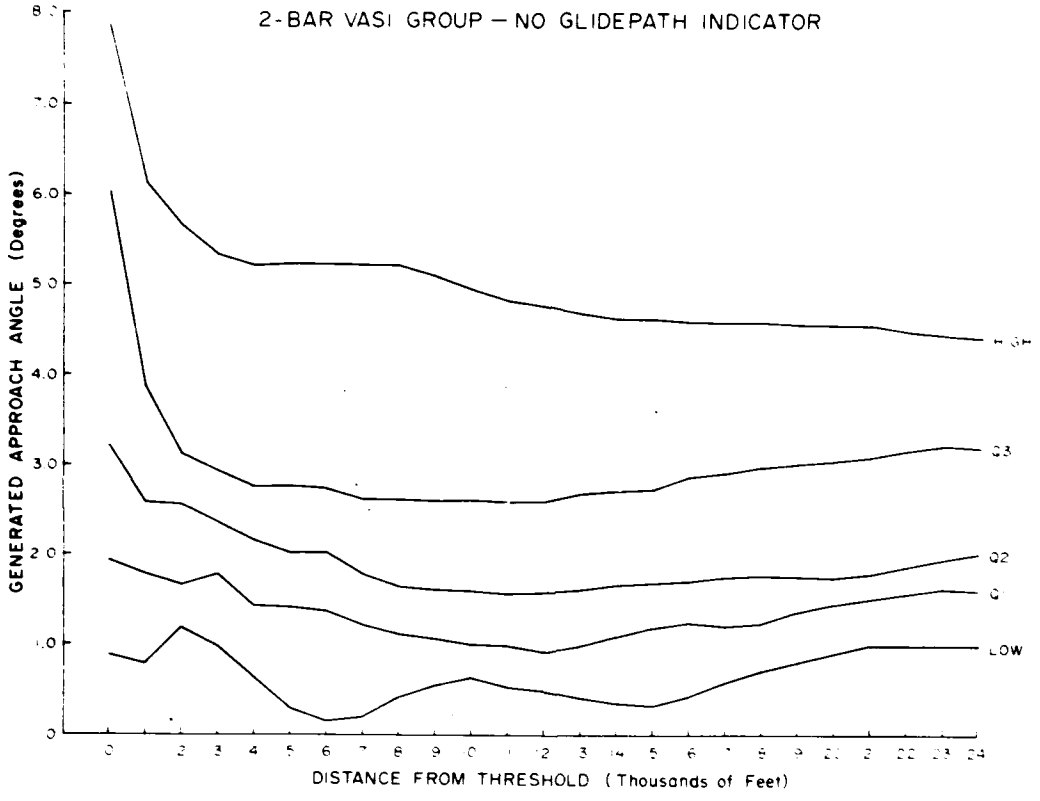

Figure 17. High scores, low scores, and quartiles of generated approach angle distributions at 1,000-ft distance intervals on no-indicator approaches by pilots of the 2-bar VASI group.

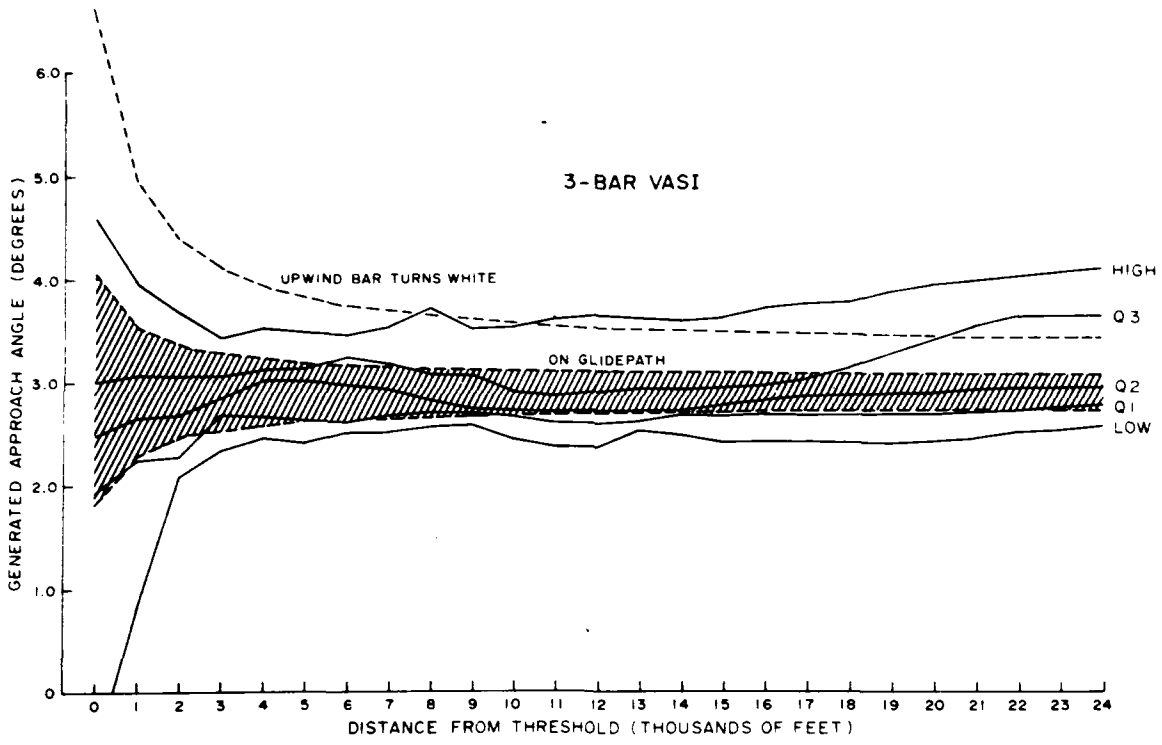

Figure 18. High scores, low scores, and quartiles of generated approach angle distributions at 1,000-ft distance intervals on approaches in which the 3-bar VASI was utilized. The range of generated approach angles that would be within the glidepath is indicated by the hatched area. The dashed line indicates the transition point from red to white in the upwind light unit.

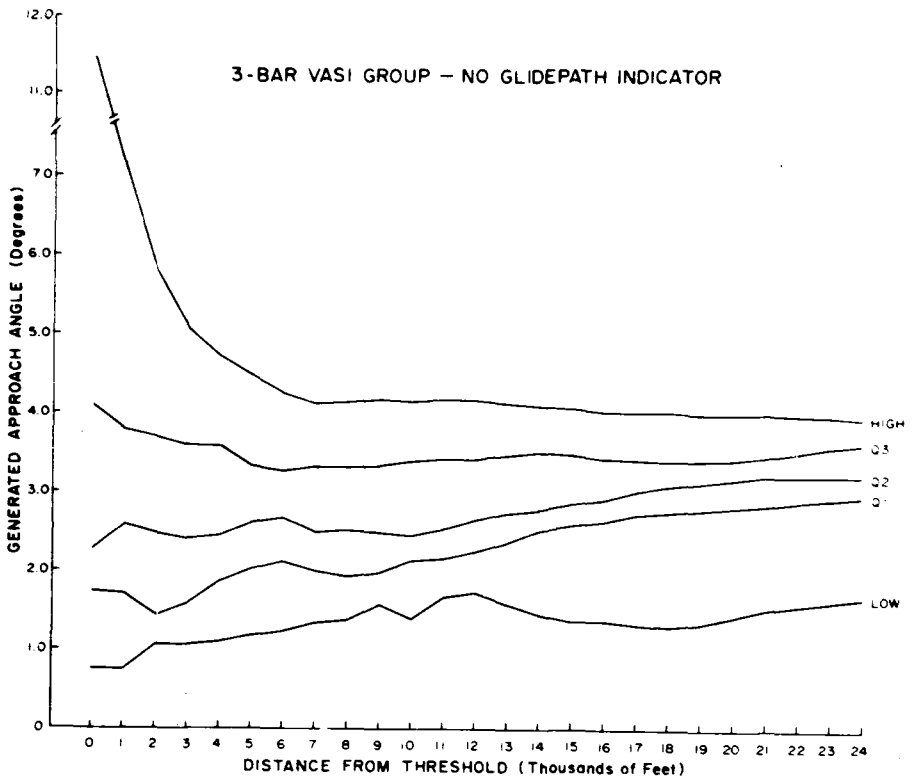

Figure 19. High scores, low scores, and quartiles of generated approach angle distributions at 1,000-ft distance intervals on no-indicator approaches by pilots of the 3-bar VASI group.

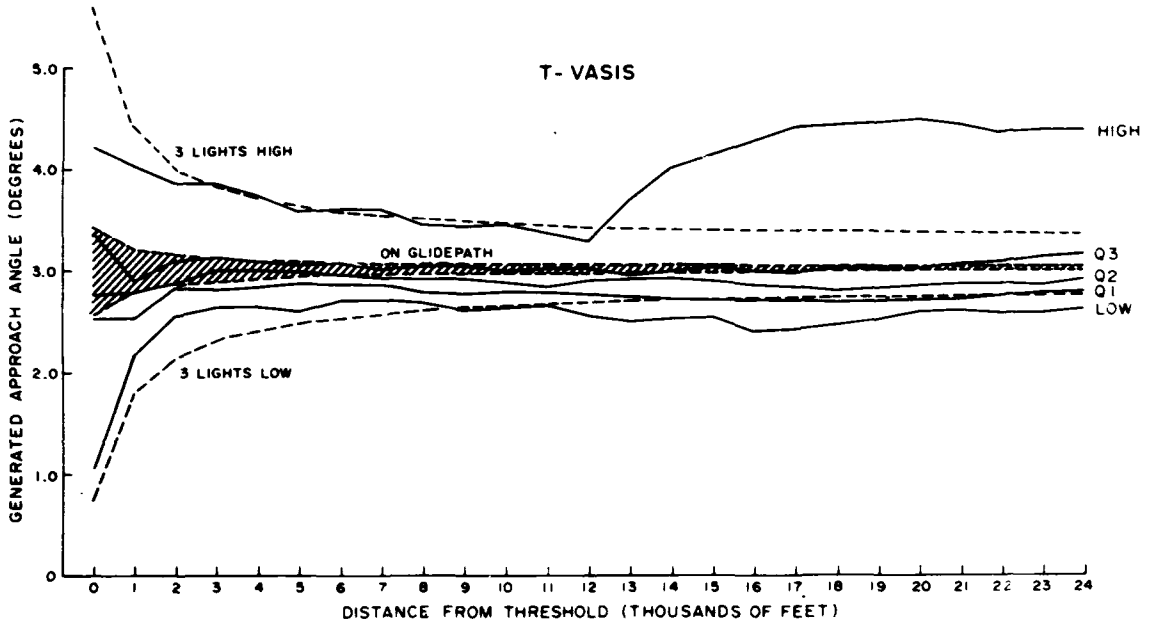

Figure 20. High scores, low scores, and quartiles of generated approach angle distributions at 1,000-ft distance intervals on approaches in which the T-VASIS was utilized. The range of generated approach angles that would be between the one-light high and one-light low signals is indicated by the hatched area. Angles at which the third light unit appears in high and low signals are indicated by dashed lines.

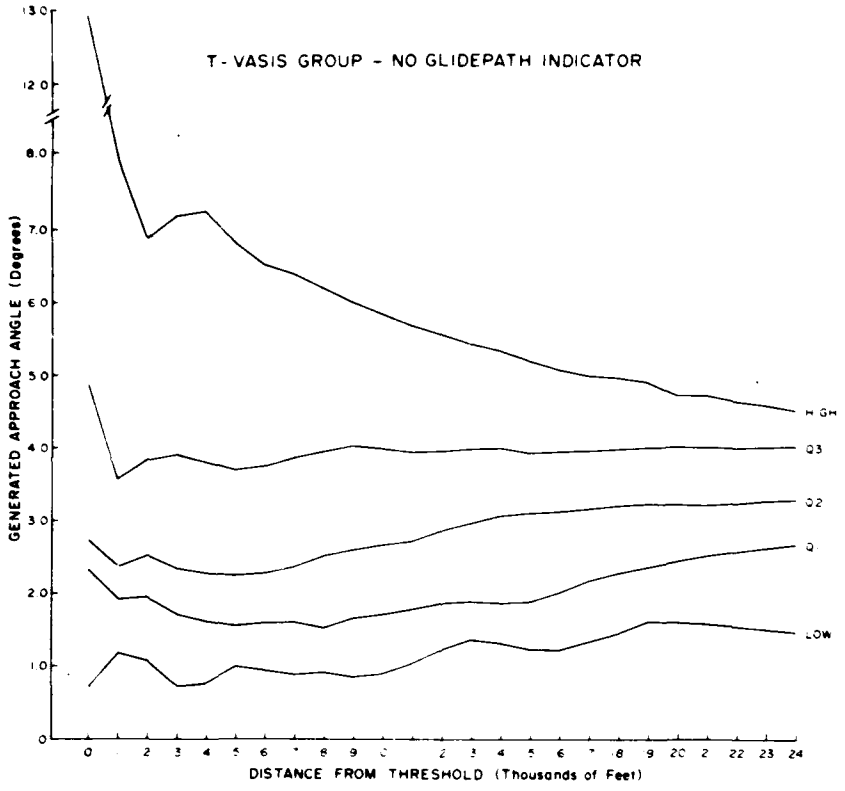

Figure 21. High scores, low scores, and quartiles of generated approach angle distributions at 1,000-ft distance intervals on no-indicator approaches by pilots of the T-VASI group.

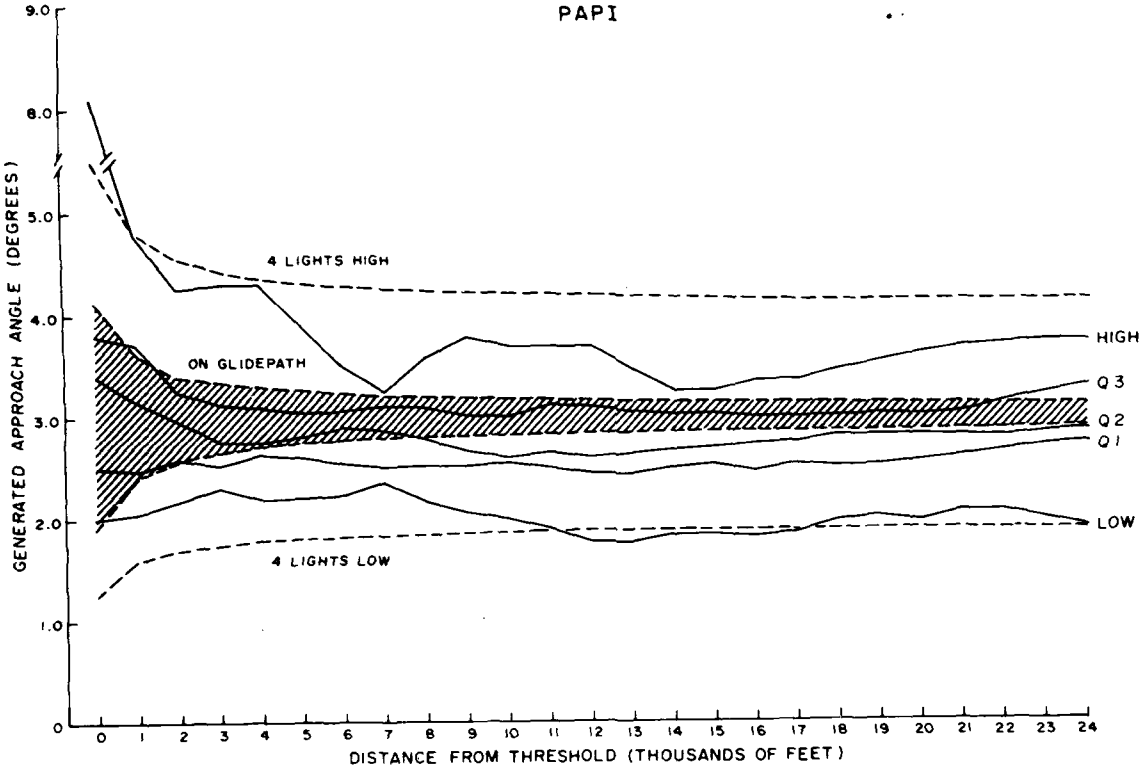

Figure 22. High scores, low scores, and quartiles of generated approach angle distributions at 1,000-ft distance intervals on approaches in which the PAPI was utilized. The range of generated approach angles between one red light in the downwind bar (low) and one white light in the upwind bar (high) is indicated by the hatched area. The angles at which the upwind bar becomes all white and the downwind bar becomes all red are indicated by dashed lines.

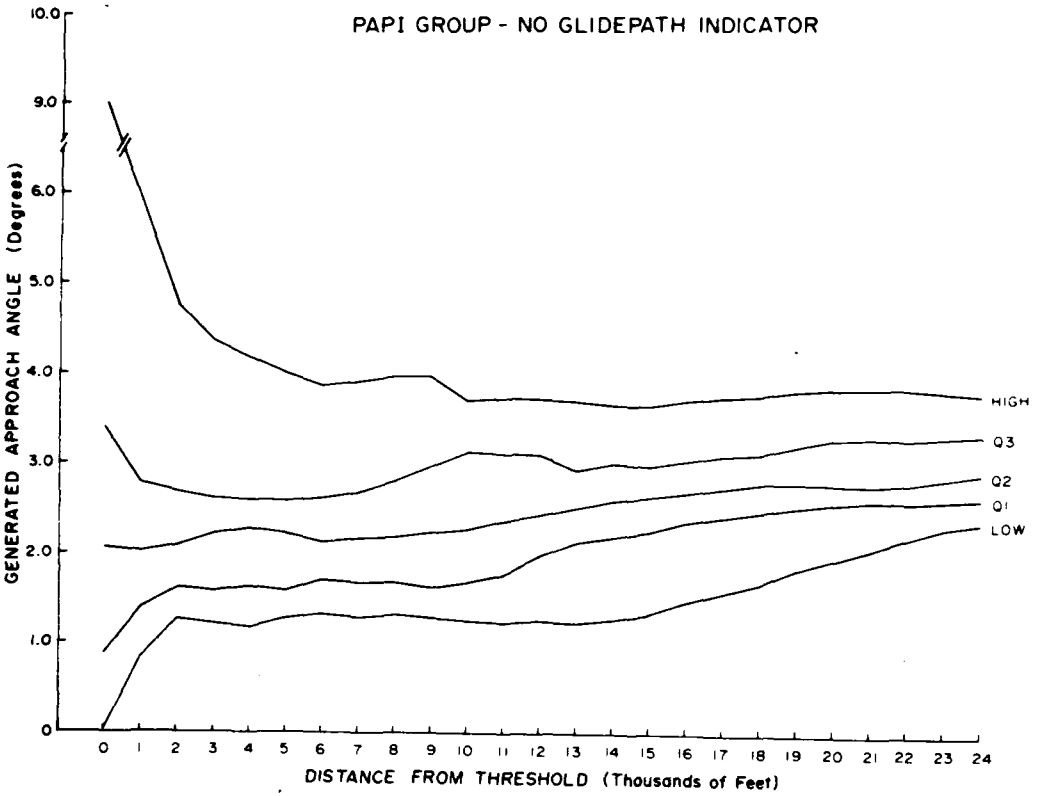

Figure 23. High scores, low scores, and quartiles of generated approach angle distributions at 1,000-ft intervals on no-indicator approaches by pilots of the PAPI group.

EXPERIMENT II

Experiment I demonstrated that pilots making simulated approaches using the T-VASIS performed better than pilots making approaches using the Red/White 2-bar VASI. Experiment II was directed towards the determination of the efficiency of these two systems in terms of their effects on pilot observing behavior. The rate at which a pilot looks at a given glidepath indicator is one measure of the importance of that indicator to safe flight. An indicator designed to facilitate safe approach and landing performance can be of utility only if the pilot looks at the indicator. From previous research on observing behavior it is well known that one factor that influences the rate of observation of a given stimulus is the rate of information change that the stimulus presents. Since, for a given approach slope, the T-VASIS presents more information (magnitude of deviation as well as direction) and at a higher rate of change than does the 2-bar VASI, it would not be unexpected for the observing response rates for these two systems to differ in favor of the T-VASIS.

Method.

Subjects. Three men with instrument and/or multiengine ratings served as subjects. All had at least 20/30 visual acuity at the distances of 30 and 40 inches and showed no evidence of color vision defect when screened by the tests described in Experiment I.

Apparatus. The apparatus was the same as in Experiment I. Only the 2-bar VASI and the Australian T-VASIS were simulated.

Procedure. Each subject was tested in four 2-hour sessions with each type of glidepath indicator in counterbalanced order. Two practice sessions were given with each type of indicator before test sessions began. In every practice and test session, eight approaches were flown with only one type of glidepath indicator. The flight plan for each mission consisted of takeoff and climb on a north heading to 2,500 ft altitude. At that altitude the simulated position of the aircraft was moved by means of computer commands to a position 50,000 ft south of the runway threshold on the extended centerline of the runway. As before, east-west travel of the simulator was fixed.

During the first practice session with each type of indicator, the indicator was turned on and was visible throughout the approach. During subsequent sessions with each type of indicator, the indicator was turned off. During approaches the indicator became visible for 1-second periods each time the pilot pressed a button on the control column. Thus, each button depression defined an observing response. In addition to recording aircraft altitude and distance at 1-second intervals, a separate record was maintained of these same variables each time an observing response occurred.

Results.

Observing responses were counted for each half-mile segment of all simulated approaches from a distance of 24,000 ft to 0 ft from runway threshold. These data are summarized in Figure 24.

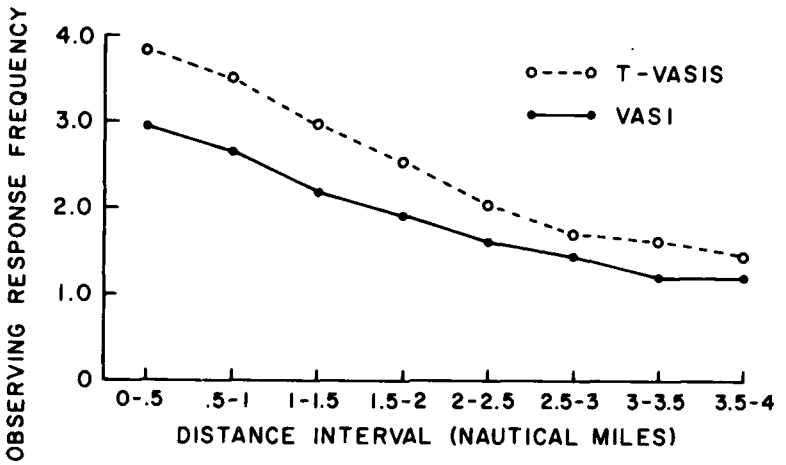

Figure 24. Frequency of observing responses in 2-bar VASI and T-VASIS approaches as a function of distance.

The analysis of variance of observing response frequency as a function of indicator type, trials, and distance indicated that the main effects of indicator type and distance were statistically significant ($p < 0.01$ for both). Both effects are clearly visible in Figure 24. Observing response frequencies were consistently higher for all subjects and at all distances with the T-VASIS than with the 2-bar VASI. Frequencies varied from approximately 20 percent higher with the T-VASIS at the 4-nautical-mile distance to approximately 30 percent higher at runway threshold on the average. The effect of distance was also large. Observing response frequency more than doubled as distance decreased from 4 nautical miles to runway threshold.

RMS altitude deviations from the 3° glidepath were also analyzed as a function of indicator type, trials, distance, and subjects. There were significant main effects of indicator type, trials, distance, and subjects, and significant first-order interactions between indicator type and trials and between indicator type and distance. All effects were significant at the $p < 0.01$ level. The main effects and interactions of indicator type and distance are illustrated in Figure 25.

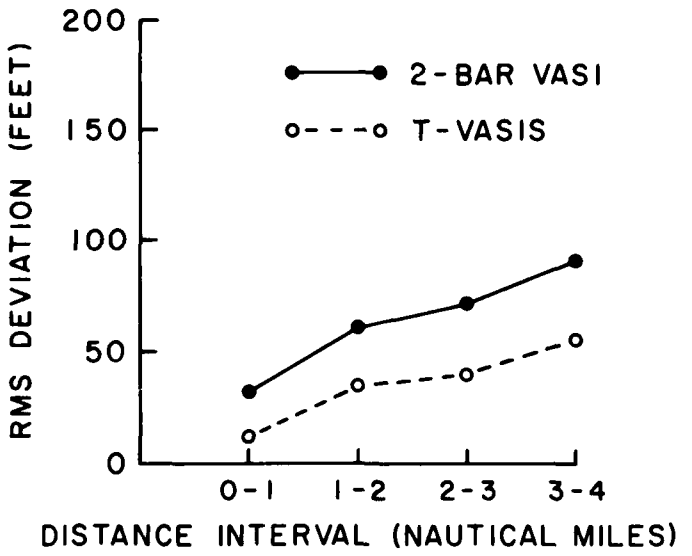

Figure 25. RMS altitude deviations on 2-bar VASI and T-VASIS as a function of distance.

Although altitude deviations decreased with distance, they did not decrease in proportion to distance, so that deviations increased when expressed in terms of generated approach angle as shown in Figure 26, which also illustrates differences among subjects.

Large effects of indicator type occurred with subjects 1 and 3. The effect was in the same direction but of lesser magnitude in subject 2, who also had the highest experience level in terms of total flying hours. The interaction of indicator type with trials did not appear to represent important long-term trends over the 16 trials and will not be discussed further.

Flight path oscillations were measured and analyzed as in Experiment I as a function of indicator type, trials, and subjects. This analysis revealed that only differences between subjects ($p < 0.01$) were significant. Oscillations are plotted as a function of indicator type and subjects in Figure 27.

Flight path oscillations did not appear to be correlated with deviations from the 3^{o} glidepath.

Descriptive statistics are presented in Tables 10 and 11 to describe distributions of generated altitude values as a function of indicator type and distance. Each value in the tables is based on 48 approaches, 16 by each of three subjects. Again, variability of distributions of T-VASIS approaches was less than that of the 2-bar VASI approaches.

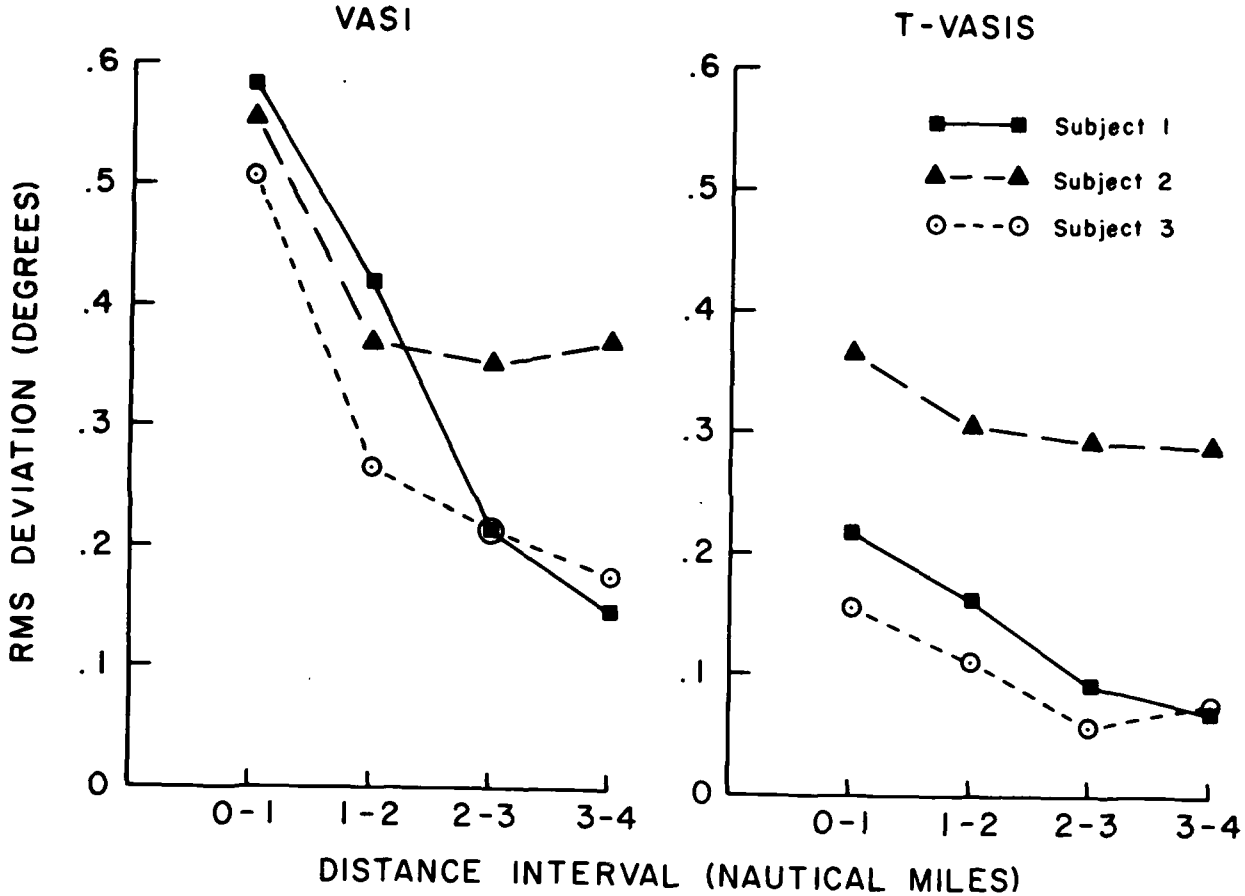

Figure 26. RMS generated approach angle deviations on 2-bar VASI and T-VASIS approaches as a function of distance for each subject.

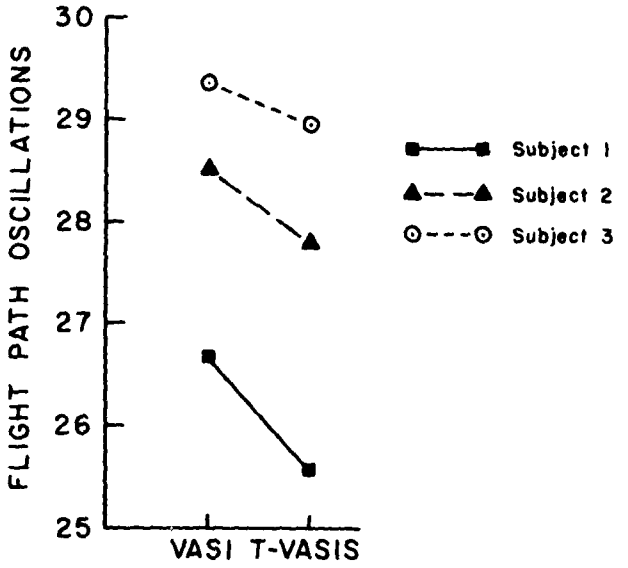

Figure 27. Flight path oscillations on 2-bar VASI and T-VASIS approaches for each subject.

Generated altitude highs, lows, and quartiles from Tables 10 and 11 were converted to generated approach angles and plotted as a function of distance in Figures 28 and 29. Comparison of these figures for the more highly practiced subjects of Experiment II with Figures 16 and 20 for the 2-bar VASI and T-VASIS conditions of Experiment I shows that variability in approaches was lower at most distances for the subjects of Experiment II. The most notable difference was the relative lack of deviations below 2° in Experiment II as compared with Experiment I in approaches with the 2-bar VASI.

Discussion.

The significant findings of these studies may be summarized as follows: During simulated approaches and landings, pilots deviated less from the ideal (3°) glidepath when making approaches with the Australian T-VASIS. Deviations in the other three glidepath indicator groups increased in the order: 3-bar VASI, PAPI, and 2-bar VASI. Deviations with the T-VASIS were significantly smaller than with the 2-bar VASI. Although performance with the T-VASIS, 3-bar VASI, and PAPI decreased in that order, there were no statistically significant differences among these groups. Deviations in both the 3-bar VASI and PAPI were found significantly smaller than in the 2-bar VASI group only in the more sensitive analysis of the generated approach angle deviations from the 3° glidepath. The present findings concerning approach performance with the T-VASIS and 2-bar VASI are in agreement with previous evaluations

TABLE 10. Experiment II: Descriptive Statistics on 48 Approaches Made With the 2-Bar VASI

DISTANCE (FT/1000)	Q1	Q2	Q3	HIGH	LOW	RANGE	MEAN	SD	SKEWNESS	KURTOSIS
THRESHOLD	33.2	40.5	46.5	53.5	16.9	66.9	40.8	13.3	0.74606	3.96061
1	71.2	79.3	91.7	115.9	53.6	62.3	82.4	[illegible]	0.49555	2.62407
2	117.6	132.0	146.0	177.2	102.8	74.4	132.8	18.4	0.32817	2.32977
3	163.8	178.0	199.4	228.8	145.6	83.2	182.0	21.9	0.36156	2.00187
4	212.1	223.7	251.3	280.3	183.1	97.2	230.3	24.8	0.26333	2.08901
5	258.7	270.3	297.7	333.4	209.1	124.3	276.3	28.3	0.12069	2.41436
6	301.3	317.2	346.3	392.9	259.2	133.7	322.9	31.2	0.21913	2.27729
7	345.3	365.4	395.4	445.6	310.0	135.6	371.0	34.7	0.26206	2.19604
8	387.9	417.7	443.7	500.1	346.8	153.3	419.3	38.1	0.16466	2.24903
9	435.2	465.3	494.2	558.4	391.9	166.5	466.5	41.9	0.14201	2.24807
10	478.9	513.9	547.9	620.3	433.2	187.1	513.2	46.0	0.10144	2.26859
11	520.2	568.6	599.5	684.7	473.2	211.5	561.7	50.6	0.03770	2.34206
12	565.8	622.2	661.1	743.5	504.4	239.1	614.0	56.7	-0.14966	2.15311
13	609.6	686.1	712.9	814.5	541.6	272.9	668.2	62.4	-0.21546	2.31860
14	672.9	744.5	779.0	881.7	581.4	300.3	724.7	68.1	-0.31117	2.41653
15	720.0	782.9	832.8	943.2	621.8	321.4	777.7	71.4	-0.33749	2.52335
16	774.6	830.0	886.3	982.2	668.6	313.6	829.7	71.4	-0.39967	2.51627
17	836.0	884.4	933.9	1009.0	727.6	281.4	879.8	69.9	-0.39139	2.32523
18	882.2	930.5	984.0	1041.7	790.7	251.0	927.9	70.5	-0.37620	2.14317
19	915.6	979.0	1036.5	1092.7	841.8	250.9	975.0	72.5	-0.32210	1.96576
20	954.3	1023.0	1088.3	1151.4	879.9	271.5	1022.4	75.9	-0.25665	1.87335
21	1007.5	1077.6	1141.6	1214.1	921.2	292.9	1070.5	80.0	-0.22387	1.84869
22	1050.2	1132.6	1194.2	1270.8	961.6	309.2	1119.8	84.9	-0.25196	1.82462
23	1084.6	1185.0	1244.0	1325.3	998.4	326.9	1166.8	89.4	-0.29127	1.84648
24	1123.4	1237.0	1294.6	1375.5	1047.0	328.5	1216.4	92.9	-0.25954	1.81170

TABLE 11. Experiment II: Descriptive Statistics on 45 Approaches Made With the T-VASIS

DISTANCE (FT/1000)	Q1	Q2	Q3	HIGH	LOW	RANGE	MEAN	SD	SKEWNESS	KURTOSIS
THRESHOLD	42.3	46.4	49.8	65.4	28.7	36.7	46.4	7.1	0.18287	3.73075
1	90.6	95.4	101.0	111.0	67.9	43.1	95.3	8.2	-0.70293	4.28946
2	143.6	150.5	153.9	165.4	112.0	53.4	148.6	9.4	-1.34977	6.27631
3	193.0	202.7	206.7	222.0	147.9	74.1	199.7	11.9	-1.71576	8.75495
4	248.2	254.3	259.1	274.9	192.0	82.9	251.9	14.1	-1.83603	8.58971
5	297.2	305.4	310.5	329.5	232.6	96.9	301.3	18.4	-2.00788	8.00030
6	340.9	356.2	362.3	385.7	273.4	112.3	348.9	23.1	-1.74520	6.28705
7	390.4	404.7	416.7	431.3	312.4	118.9	398.4	26.5	-1.54440	5.35594
8	435.9	450.6	465.4	485.5	353.0	132.5	445.9	28.1	-1.41456	5.15610
9	480.5	496.0	510.3	542.2	391.6	150.6	491.9	30.3	-1.40686	5.56881
10	528.4	548.7	559.8	607.9	422.9	185.0	539.9	35.8	-1.36359	5.82445
11	582.5	597.7	614.8	670.3	451.5	218.8	591.1	43.9	-1.25248	5.35823
12	636.9	657.7	673.6	733.0	479.6	253.4	647.7	50.7	-1.55079	5.80826
13	693.1	714.2	725.1	793.0	515.3	277.7	703.3	55.2	-1.69880	6.40751
14	756.1	777.4	788.5	858.9	559.1	299.8	763.4	59.8	-1.86355	6.79113
15	819.0	832.4	846.2	908.8	610.7	298.1	820.0	62.8	-2.01685	7.07664
16	874.4	883.0	895.6	952.3	659.0	293.3	872.0	63.8	-2.13348	7.45712
17	920.7	936.3	951.2	1013.4	692.2	321.2	922.6	68.6	-2.20370	7.66170
18	968.7	990.3	1004.3	1078.2	739.5	338.7	973.5	73.5	-2.10697	7.13578
19	1018.1	1041.0	1062.8	1129.8	761.7	368.1	1024.6	80.8	-2.05939	6.88471
20	1072.6	1093.5	1118.1	1187.8	787.9	399.9	1076.8	86.2	-1.99705	6.66129
21	1120.1	1145.6	1168.1	1250.2	837.5	412.7	1127.1	88.6	-1.85466	6.22780
22	1165.3	1196.9	1212.0	1324.9	900.8	424.1	1176.4	90.4	-1.58064	5.51030
23	1209.9	1244.4	1276.6	1395.0	952.4	442.6	1225.3	93.5	-1.38155	5.05180
24	1255.1	1291.5	1332.0	1450.8	994.4	456.4	1274.6	98.7	-1.26870	4.68748

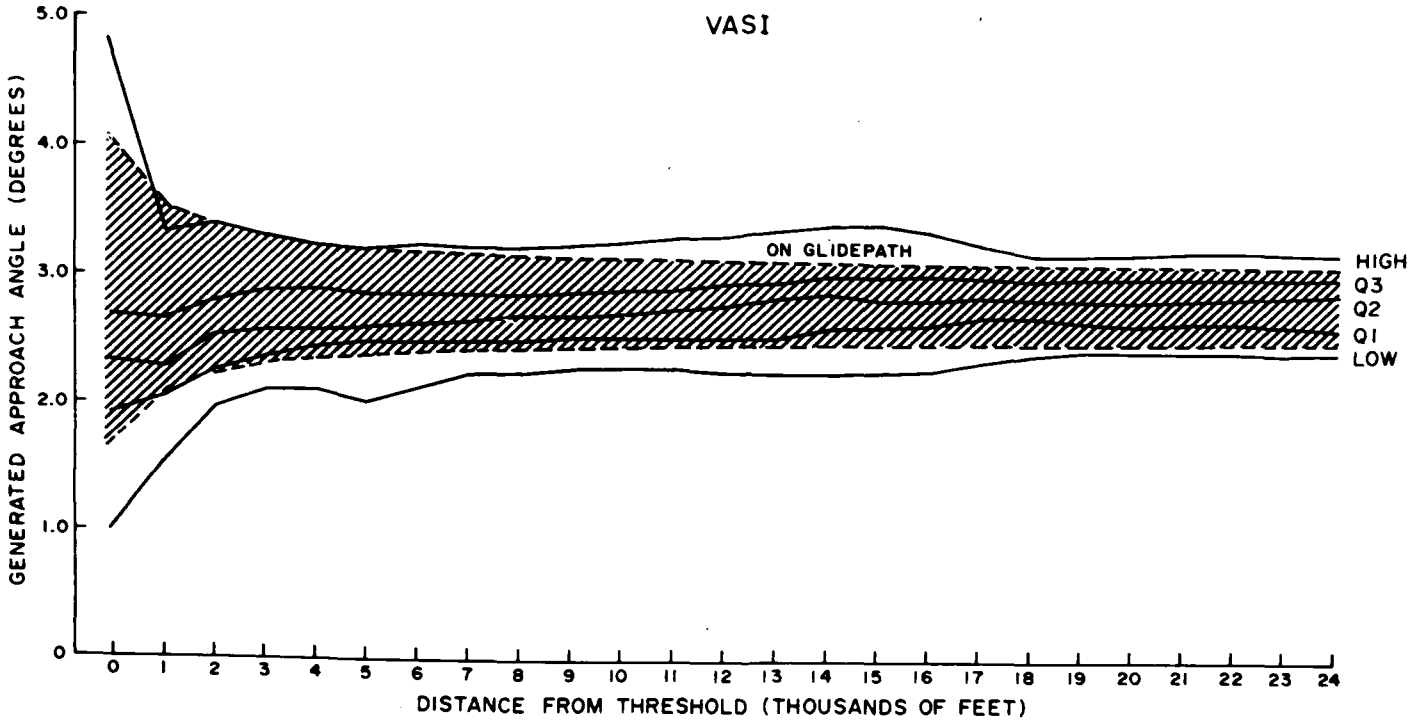

Figure 28. High scores, low scores, and quartiles of generated approach angle distributions at 1,000-ft distance intervals on 2-bar VASI approaches in Experiment II.

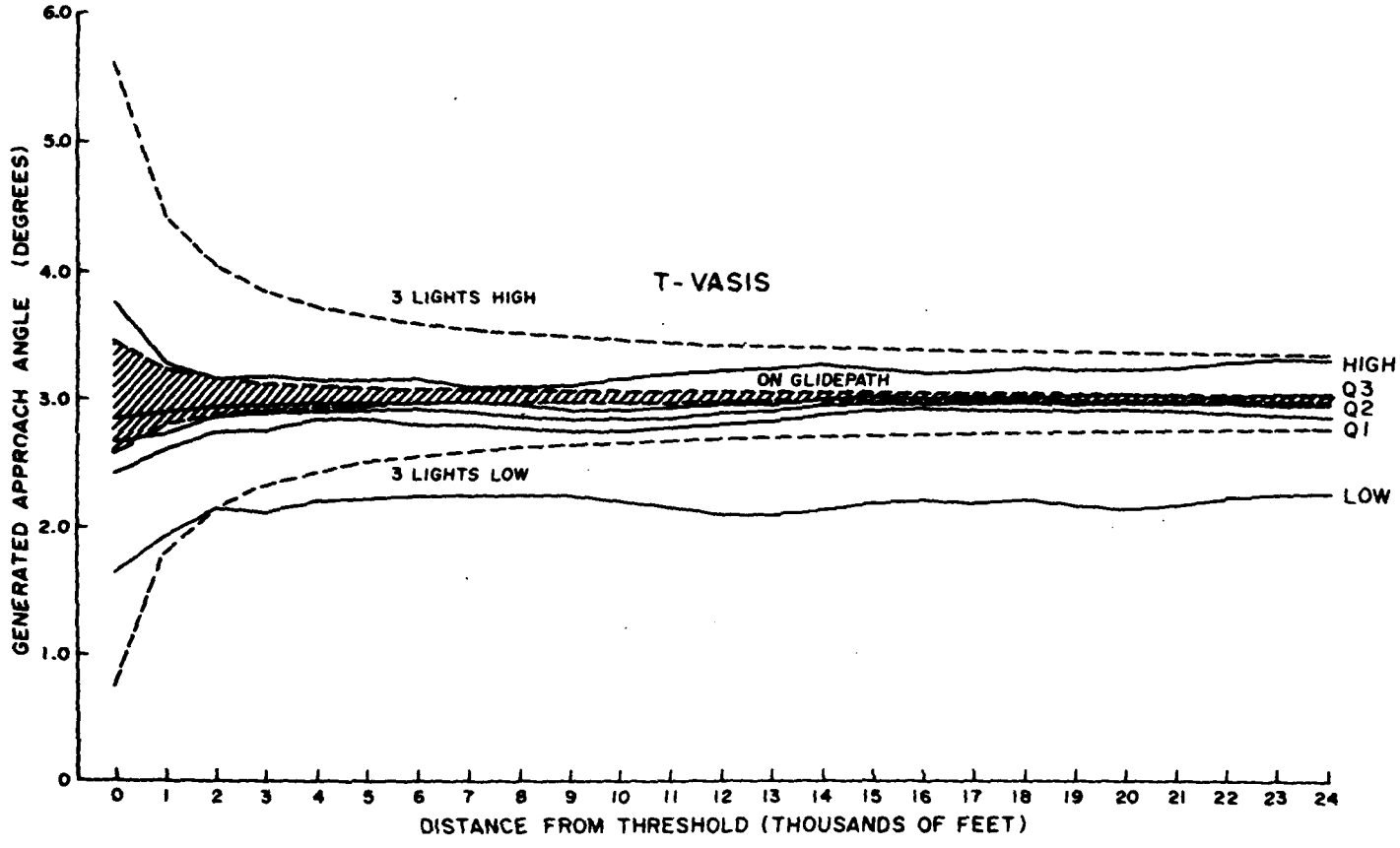

Figure 29. High scores, low scores, and quartiles of generated approach angle distributions at 1,000-ft distance intervals on T-VASIS approaches in Experiment II.

(2,4) of these glidepath indicators, studies which also found the T-VASIS superior in terms of reducing deviation from the desired approach path. In one of these studies (2) which presented data in comparable form, RMS deviations from the ideal glidepath with both systems were approximately one-half the magnitude of deviations found in the present study. This probably can be attributed to the present study's use of pilots who were not required to have type-ratings in the simulated aircraft and to the drastically and deliberately reduced visual information presented in the current experiments. The second experiment replicated the finding that approach and landing performance with the T-VASIS was superior to performance with the 2-bar Red/White VASI and demonstrated that pilots make more observing responses with the T-VASIS than with the Red/White VASI.

All glidepath indicators greatly reduced deviations from the desired 3° glidepath in the simulated nighttime conditions in which cues from runway lighting were the only other extra-cockpit source of visual information for vertical guidance. In all four groups of pilots, when no ground-based glidepath indicator was present, approaches tended to be low on the average, with dangerously low approaches occurring in some cases. These data involving simulated night approaches give empirical support to previous demonstrations of similar illusions in laboratory situations (8,11) and anecdotal reports of illusions in the perception of approach angle during actual approaches. This finding clearly suggests the great importance of ground-based glidepath indicators for night approaches, especially when "black hole" conditions exist.

The higher frequency of observing responses obtained with the T-VASIS was not unexpected. The higher rate of change of information presentation predicts such a finding and together with the superior performance with the T-VASIS suggests that observing response rate is a significant factor in performance of safe landings.

Consider an aircraft that begins an approach with a glidepath slightly steeper than the 3° ideal. Unless corrected, such a glidepath will result in a short landing. As indicated in Figure 1, however, only two changes in appearance of the Red/White VASI occur: the first is a change from a WHITE-over-WHITE aspect to a RED-over-WHITE aspect as the aircraft penetrates the envelope defined by the VASI's cutoff angles. At this point the VASI indicates "on glidepath" when, in fact, the aircraft is making a too steep approach. As the aircraft continues to descend through the envelope, the VASI continues to display the "on glidepath" aspect. Since the information presented by the VASI does not change as the descent continues within the envelope, we would expect the frequency with which the pilot observes the VASI to decrease. As a consequence it is possible for the pilot to fail to make an observing response (i.e., "attend" to the VASI) when the lower limit of the envelope is finally penetrated and the VASI indicates "too low" (RED-over-RED). Indeed, we would predict that approaches would occasionally result in just such a profile and with a resultant short landing if cues in the runway image

failed to provide adequate vertical guidance at the same time. This seems likely to happen on occasions in view of the literature concerning the high accident rate in night visual approaches, a rate that has been attributed to visual illusions involving a perceptual tendency to overestimate altitude or angle of approach at night (3,7,9).

Now consider the same aircraft beginning the same "slightly too steep" approach with the T-VASIS. As indicated in Figure 3, a comparatively high rate of information change occurs as the aircraft descends. The relatively rapid change in the visual aspect presented by the T-VASIS makes it much more likely that the pilot will make an observing response and check the descent. In other words, the same analysis that would predict some approaches to result in short landings with the Red/White VASI would predict that significantly fewer approaches with the T-VASIS will result in short landings.

Frequency of responding to the glidepath indicator for vertical guidance may not be the only problem in the use of glidepath indicators. After receiving a low signal from the glidepath indicator, the pilot, in order to maintain a relatively stable flight, is likely to make a flight path correction by reducing rate of descent rather than by eliminating further descent. It is possible that the reduction in rate of descent would be insufficient to make the flight path intersect the visual glidepath of the indicator. Unless the pilot receives rapid feedback from the indicator concerning the adequacy of his correction, he may continue a low approach. The T-VASIS and the PAPI are designed so that if descent below the desired glidepath continues, feedback is provided so that additional flight path corrections can be made. After once deviating below the 2- and 3-bar VASI glidepaths, no further information about change of position relative to the visual glidepath is presented unless the correction is sufficient to make the flight path intersect the VASI glidepath. This might be an especially important problem if downdrafts were present. The pilot's strategy in the use of glidepath indicators is very important and obviously must involve careful integration of information from the glidepath indicator on the ground with information provided by altitude and vertical speed indicators. Quantitative information about deviation below the desired glidepath as provided by the T-VASIS and the PAPI would seem to be very helpful in this integration process.

It should be noted, however, that the same theoretical analysis that predicts superior performance with the T-VASIS also predicts superior performance with the PAPI. Both systems share the characteristic of presenting quantitative information about deviation from ideal glidepath in addition to the directional information presented by all systems studied. (To some extent the 3-bar VASI can be regarded as presenting some quantitative information about deviations above the ideal glidepath for pilots using the downwind pair of bars and some quantitative information about deviations below the ideal for pilots of large-bodied transports. It could be argued that the intermediate performance obtained by using the 3-bar VASI was due to the presence of this information.) It is apparent then that the presence of additional information in a glidepath indicator is not a sufficient condition for superior performance,

since the PAPI group was not superior to the 3-bar VASI group. It appears possible that the ease with which pilots interpret the information displayed is an important factor. Thus, the T-VASIS presents an easily interpreted "T" that tells the pilot to fly in the direction indicated: fly up for the normal "T"--fly down for the inverted "T." The PAPI may not be as easily interpreted and may require greater experience before a pilot becomes proficient in readily interpreting the information encoded in the lights. Another possible reason for the differences between T-VASIS and PAPI approaches may be the difference in precision of information (size of approach angle steps between cutoff angles of adjacent light units). However, the failure of the PAPI to prove superior to the 2-bar VASI argues against this second interpretation.

The failure of the PAPI system to prove significantly superior to the 3-bar VASI system was unexpected in view of prior reports to the contrary (5,12,14). This discrepancy is hard to evaluate since existing reports about the PAPI do not present data other than a very small number of illustrative profiles of approaches with the PAPI and VASI (14) or subjective evaluations of pilots (5,12); no quantitative data are presented. Further research would seem appropriate to resolve this apparent discrepancy. The absence of the pink zone in simulated Red/White VASI and PAPI units in the present simulation should not have adversely affected performance in the PAPI condition, since the PAPI light units have very sharp transition zones (2 min of arc or less) that would provide an almost instantaneous change of color as did the present simulation. The similarity between 3-bar VASI and PAPI systems regarding angular width of the visually defined glidepath, shown by the hatched areas in Figures 18 and 22, may be one reason that performance did not differ substantially between these groups. With the exception of the relation between these two groups, performance with the four indicator systems is correlated with the angular width of the visual glidepath defined by the particular system as can be seen in Figures 16, 18, 20, and 22. This finding suggests that the effectiveness of the standard 2-bar VASI might be improved by reducing the 0.50° difference between cutoff angles of upwind and downwind light units to the 0.25° of the 3-bar VASI system, or perhaps to an even smaller value. It should be noted that a second version of the PAPI has only one row of light units (10); this later version was not included in the current study, because the report describing it was received after the present experiment was completed.

With regard to the simulated 2-bar and 3-bar VASI systems, the absence of the pink zone in simulated light units might decrease performance relative to the real world system, if the pink zone does provide some quantitative information about deviation from VASI glidepath as pilots suggest (See appendix). Nevertheless, the relative performance in 2-bar VASI and T-VASIS conditions of the present experiment was similar to that found by Baxter, Cumming, Davy, and Lane (2) with real 2-bar VASI and T-VASIS systems. In both studies RMS altitude deviations were about two times greater with the 2-bar VASI than with the T-VASIS over the distance range of 0 to 4 nautical miles from threshold, with a tendency for the advantage of the T-VASIS to

increase as distance from threshold decreased. The ratio of RMS altitude deviations in 2-bar VASI and T-VASIS conditions was 1.74 in the nighttime data of Baxter et al. and 2.06 and 1.77 in Experiments I and II, respectively, of the current study. The similarity of findings in these two studies suggests that the possible quantitative information in the pink zone may not be a very effective source of quantitative information and also suggests that the reduced intensity of red lights and lack of pink zone in the present simulation does not invalidate its use for the study of such systems.

The salient features of the T-VASIS are (1) presentation of quantitative information about deviation from ideal glidepath, and (2) use of a narrow cutoff angle to define the "on glidepath" envelope. These studies do not permit us to state which of these factors is more important in design of visual landing indicators. Clearly, the relative values of these features are amenable to test. (Again, note the failure of the PAPI, which also possesses these features, to prove significantly superior statistically to the 3-bar VASI, but note also the intermediate performance of the 3-bar VASI, which has narrower cutoff angles than the 2-bar and which, as indicated above, can be considered to present some quantitative information.) We recommend that any future evaluation of visual landing indicators include a test to determine the relative value of these features and also the ease of interpretation of the information presented by the various indicators under study. Strategies taught pilots for using the glidepath indicators should also be considered. The present experimental methods involving simulation do not, of course, achieve complete realism and cannot replace an ultimate operational evaluation of visual glidepath indicators. However, these methods do provide a technique for preliminary analysis of indicators in which variables such as cutoff angles and geometric configurations may be varied conveniently and reliably. New indices of performance (such as the observing responses in the present study) can be explored to identify the processes by which various glidepath indicators produce differences in approach performance.

References

1. Australian Government: T-VASIS: T-Visual Approach System. Publication No. 58, Issue 1. Air Transport Group, Department of Transport, Canberra, Australia, 1974.

2. Baxter, J. R., R. W. Cumming, R. H. Davy, and J. C. Lane: A Comparison of Three Visual Glidepath Systems. Human Engineering Note 8, Aeronautical Research Laboratories, Australian Defense Scientific Service, Department of Supply, Canberra, Australia, 1960.

3. Hasbrook, A. H.: The Approach and Landing: Cues and Clues to a Safe Touchdown. BUSINESS AND COMMERCIAL AVIATION, 32:39-43, 1975.

4. Hyman, M. L.: Comparative Evaluation of Australian TVG and United States Standard Visual Approach Slope Indicators. Final Report. Project No. 421-2V. Systems Research and Development Service, Federal Aviation Agency, Atlantic City, July 1963.

5. International Civil Aviation Organization: VASIS-Sharp Transition Glideslope Indicators. Report No. VAP/7-WP/15, Seventh Meeting of the ICAO Visual Aids Panel, February 2-20, 1976, 1000 Sherbrooke St., N.W., Montreal, PQ, Canada.

6. Jones, P. H.: VASI Improvements--"T"-VASI Evaluation. NAFEC Technical Letter Report NA-77-45-LR. National Aviation Facilities Experimental Center, Federal Aviation Administration, Atlantic City, August 1977.

7. Kendall, M. G., and A. Stuart: The Advanced Theory of Statistics. London, Charles Griffin and Co., p. 85, 1958.

8. Kraft, C. L.: Measurement of Height and Distance Information Provided by the Extra-Cockpit Visual Scene. In: Visual Factors in Transportation Systems: Proceedings of the Spring Meeting, 1969. Committee on Vision, National Academy of Sciences--National Research Council, Washington, D.C., pp. 84-101, 1969.

9. Lewis, M. F., H. W. Mertens, and T. Kempsell: A Real-Time Graphics System for RSX-11D. Proceedings of the Digital Equipment Computer Users Society, 2:441-442, 1975.

10. Lina, L. J., and G. C. Cavanos: Influence of Angle of Glide Slope on the Accuracy of Performing Instrument Approaches in a Simulator. National Aeronautics and Space Administration, Technical Note NASA TN D-4835, Washington, D. C., 1968.

11. Mertens, H. W.: Comparison of the Visual Perception of a Runway Model in Pilots and Nonpilots During Simulated Night Landing Approaches. FAA Office of Aviation Medicine Report No. AM-78-15, 1978.

12. Paprocki, T. H.: Quick Response Evaluation of Precision Approach Path Indicator (PAPI). NAFEC Technical Letter Report NA-77-36-LR. National Aviation Facilities Experimental Center, Atlantic City, July 1977.

13. Paprocki, T. H.: Abbreviated "T"-VASI Interim Report. NAFEC Technical Letter Report NA-78-33-LR. National Aviation Facilities Experimental Center, Atlantic City, May 1978.

14. Smith, A. J., and D. Johnson: The Precision Approach Path Indicator--PAPI. Technical Report 76123. Royal Aircraft Establishment, Great Britain, September 1976.

15. Stark, E. A.: Digital Image Generation: The Medium with a Message. In: Proceedings of the 1977 IMAGE Conference. Flying Training Division, Air Force Systems Command, Williams Air Force Base, Arizona, pp. 186-201, May 1977.

16. U.S. Government: Visual Approach Slope Indicator (VASI) Systems. Advisory Circular No. 150/5340-25, Federal Aviation Administration, Department of Transportation, Washington, D.C., September 1976.

APPENDIX

Subjective Assessment of Simulation

Although absolute realism may be impossible (15), visual simulation systems must strive for realism in generating the visual information that imitates "real world" situations. All simulation systems thus far developed involve deliberate compromises based on practicalities, usually involving cost and limitations of technology. It is important to recognize these compromises and their implications for the meaning of performance data derived from research utilizing these simulation systems.

One limitation common to visual simulation systems with computer-generated images is the inability to reproduce the full range of colors and light intensities that the human eye can identify. In the present system, the intensity of the red lights was lower than in actual VASI systems, and the pink zone apparent during the transition between red and white sectors of real VASI light units could not be simulated. The intensity problem was dealt with in the present experiments by questioning pilots during practice runs to make certain that the red lights of the VASI could be identified correctly at simulated distances of at least 24,000 ft from the runway. It was not possible to compensate for the lack of the pink zone. To further evaluate the importance of these departures from realism, subjects were questioned after the experiment regarding the effectiveness of the particular glidepath indicator simulated for their group.

The subjects who participated in Experiment I were asked during debriefing to compare the effectiveness of the particular indicator simulated for their group with that of the 2-bar VASI as experienced in actual approaches prior to the experiment. Subjects in the 2-bar and 3-bar VASI groups gave very similar comments and, in all but one case, indicated that the real VASI signals were preferred. The preference by 7 of the 12 subjects in the 2-bar and 3-bar VASI groups was based in part on their feeling that the simulated red lights were dimmer and harder to identify at long distances than are the red lights of the real VASI. Three subjects of these two groups stated that they missed the information provided by the real VASI's pink zone, which indicates small glidepath deviations. The one subject who preferred the simulated 3-bar VASI over the real 2-bar VASI stated that it gave more information about "how high you are."

The comments of three subjects in the 2- and 3-bar VASI groups suggest that the absence of the pink zone may represent a decrement of information which might affect performance in the simulator adversely. This factor cannot be assessed in the present data and an experimental study of the effect of the size of the pink zone would seem indicated. Although subjects felt that simulated red lights were dimmer and thus harder to identify at long distances, this dimness should not have caused a problem since performance was not

measured at distances beyond 24,000 ft from the runway, a range at which subjects were tested for ability to see the red lights.

Four subjects in the T-VASIS group and four in the PAPI group preferred these simulated indicators and stated that they provided better vertical guidance information than the real 2-bar VASI and thus made flying approaches easier. One subject in the T-VASIS group who preferred the real 2-bar VASI did so because he thought the greater sensitivity of the T-VASIS caused approaches to be more unstable. The other subject in the T-VASIS group preferred the real VASI signals with their "shades of color between red and white."

One subject in the PAPI group preferred the real 2-bar VASI because the brighter red signals of the real 2-bar VASI gave "stronger low" signals. The other subject in the PAPI group felt there was not a significant difference between the effectiveness of the simulated PAPI and that of the actual 2-bar VASI.

Although the comments of pilots suggest that the pink zone may provide quantitative information about deviation from VASI glidepath, the relative performance in T-VASIS and 2-bar VASI conditions with the present simulation was similar to that measured by Baxter et al. (2) with real 2-bar VASI and T-VASIS systems, as discussed above. This similarity of findings suggests that, in contrast to the subjective impressions of pilots, the pink zone may not constitute an important source of information in terms of performance. The effect of variation in pink zone width on performance should receive further experimental study.

Initial Test of System

To initially evaluate the visual simulation and data collection systems, a brief preliminary study was conducted to compare the relative effectiveness of the 2-bar (red/white) VASI and ILS systems in minimizing deviation from the ideal approach path. A simple demonstration of the greater precision of the ILS system relative to the VASI for control of vertical position relative to the ideal 3° glidepath was conducted.

Method.

Subjects. Six male pilots with instrument and multiengine ratings served as subjects. All subjects were screened for defective color vision with the Farnsworth Lantern. No evidence of color vision deficiencies was found.

Apparatus. All details of the apparatus and visual simulation are the same as in Experiment I.

Procedure. Details of the experimental procedure were identical to those of Experiment I with the exception that each subject flew three approaches

with the ILS and three with the VASI in counterbalanced order and that the VASI was simulated bilaterally.

Results and Discussion.

Aircraft position was recorded once per second during approaches over the distance range of 35,000 ft to runway threshold. Graphical records of flown approach paths for all landings are presented in Figures 30 through 35 for each of the six subjects. Figures 30 and 34 contain the best single approach for any pilot for ILS and VASI landings, respectively. Figures 31 and 33 contain those approaches involving the greatest deviation from the 3° glidepath of ILS and VASI landings, respectively.

ILS approaches tended to be slightly high in five of the six subjects, as shown in Figures 30 through 35. This tendency is similar to one found by Lina and Canavos (10) in ILS approaches when large jet transports were simulated. In contrast, VASI approaches of the present study were, on the average, more variable and below the ideal 3° glidepath. This effect was due to consistently large deviations flown below the 3° glidepath by three of the six subjects. The exceptionally low approach of subject 4 was probably not due to inexperience with the VASI, because two prior VASI approaches made by the subject were not extremely low. On the low approach, subject 4 did demonstrate an appropriate response to the VASI at a simulated distance of 12,000 ft from touchdown and managed to return to a safe altitude. It is not known whether this subject did not see the VASI on the extremely low approach until the 12,000-ft distance or did not interpret the signal properly. Visual illusions in the nighttime scene in which pilots tend to overestimate approach angle might make a pilot think that he was just barely under the glidepath provided by the VASI's lower boundary, when, in fact, he was much lower. In general, although VASI approaches tended to be slightly low in the last 10,000 ft, the large errors occurred at greater distances, a situation in agreement with the analysis of RMS altitude deviations in both Experiments I and II.

The expected superiority of the ILS system for vertical guidance was demonstrated and is undoubtedly due to the greater amount of information provided by the ILS concerning the aircraft's position relative to the ideal glidepath. With regard to the latter point, the VASI system indicates only if the aircraft is above, below, or within an approach corridor approximately 0.5° wide as defined by the upwind and downwind bars of the VASI. While the aircraft is within the VASI approach corridor, no information concerning deviation from the ideal glidepath is provided unless transition outside the approach corridor occurs. In contrast, the ILS provides a continuous analog picture of deviation from the ideal glidepath. This scalar display identifies the ideal glidepath more precisely and permits quicker identification of deviation than does the discrete display provided by the VASI. With the limitation that the effect of absence of the pink zone cannot be presently assessed, the present method is thought to provide a convenient and flexible system for preliminary evaluation of different concepts in development of

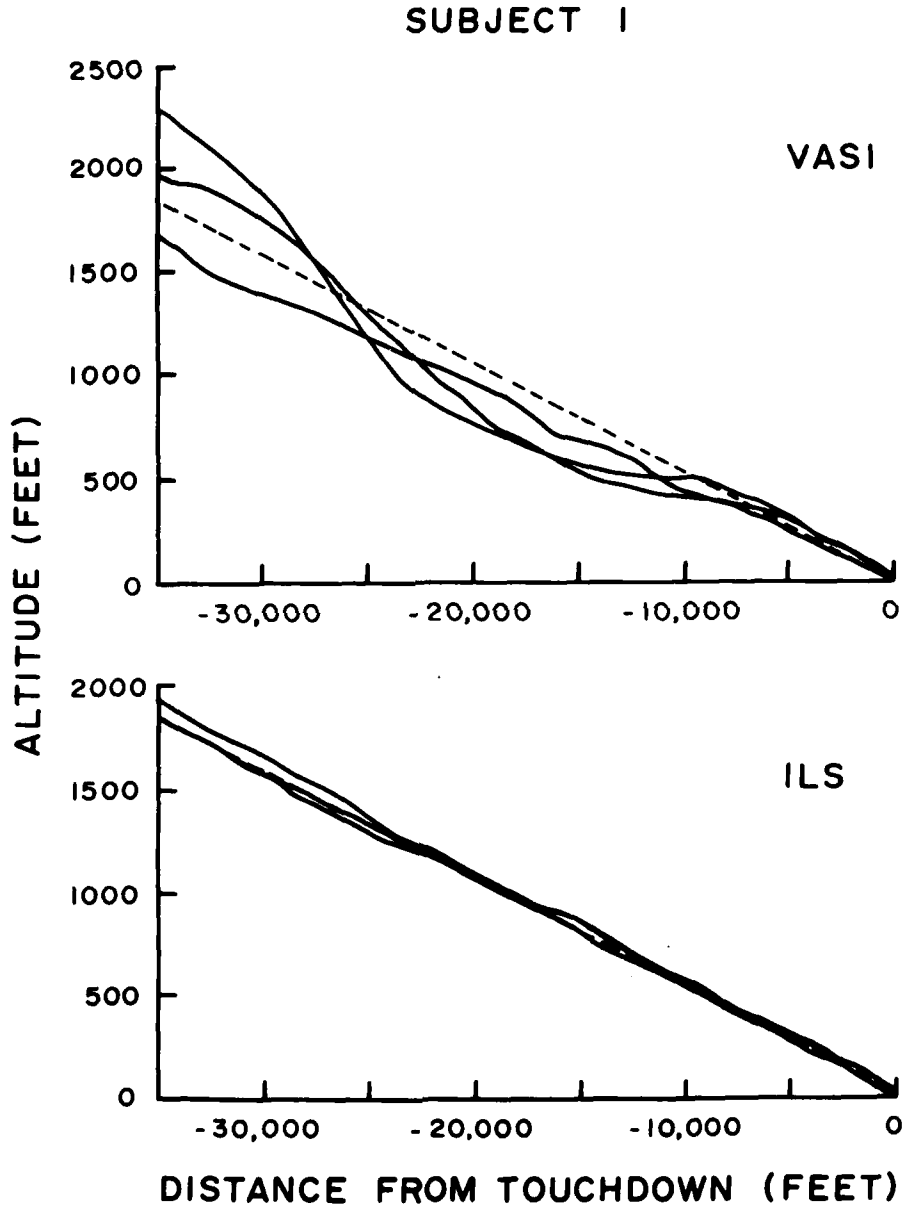

Figure 30. Approach path profiles for 2-bar VASI and ILS approaches for subject 1.

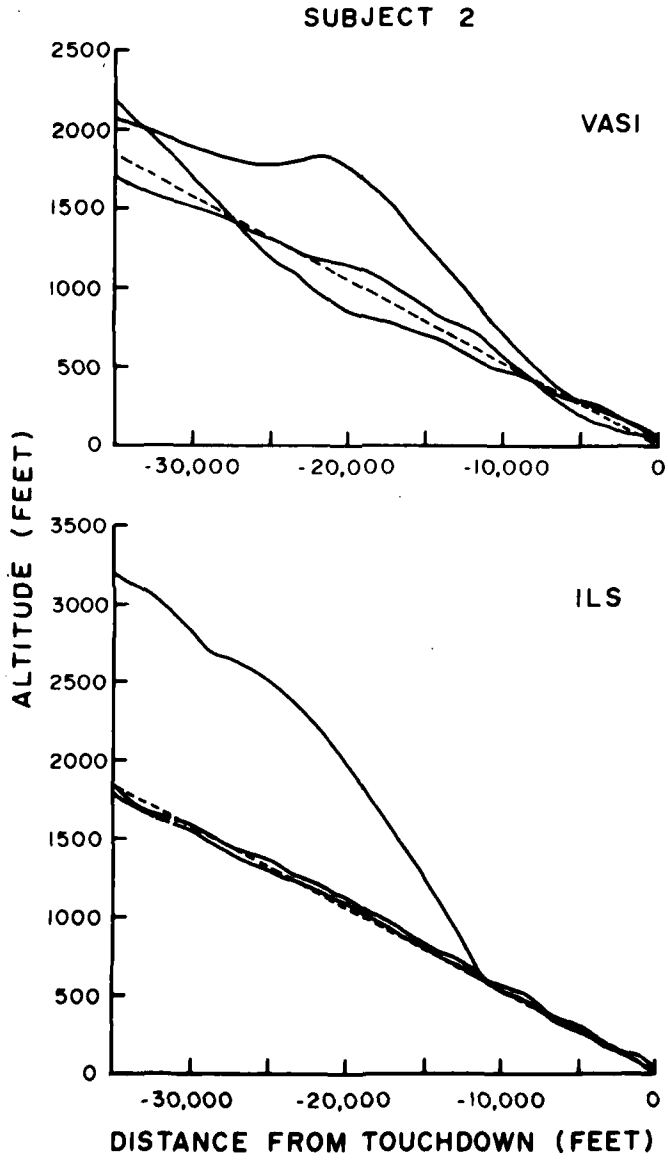

Figure 31. Approach path profiles for 2-bar VASI and ILS approaches for subject 2.

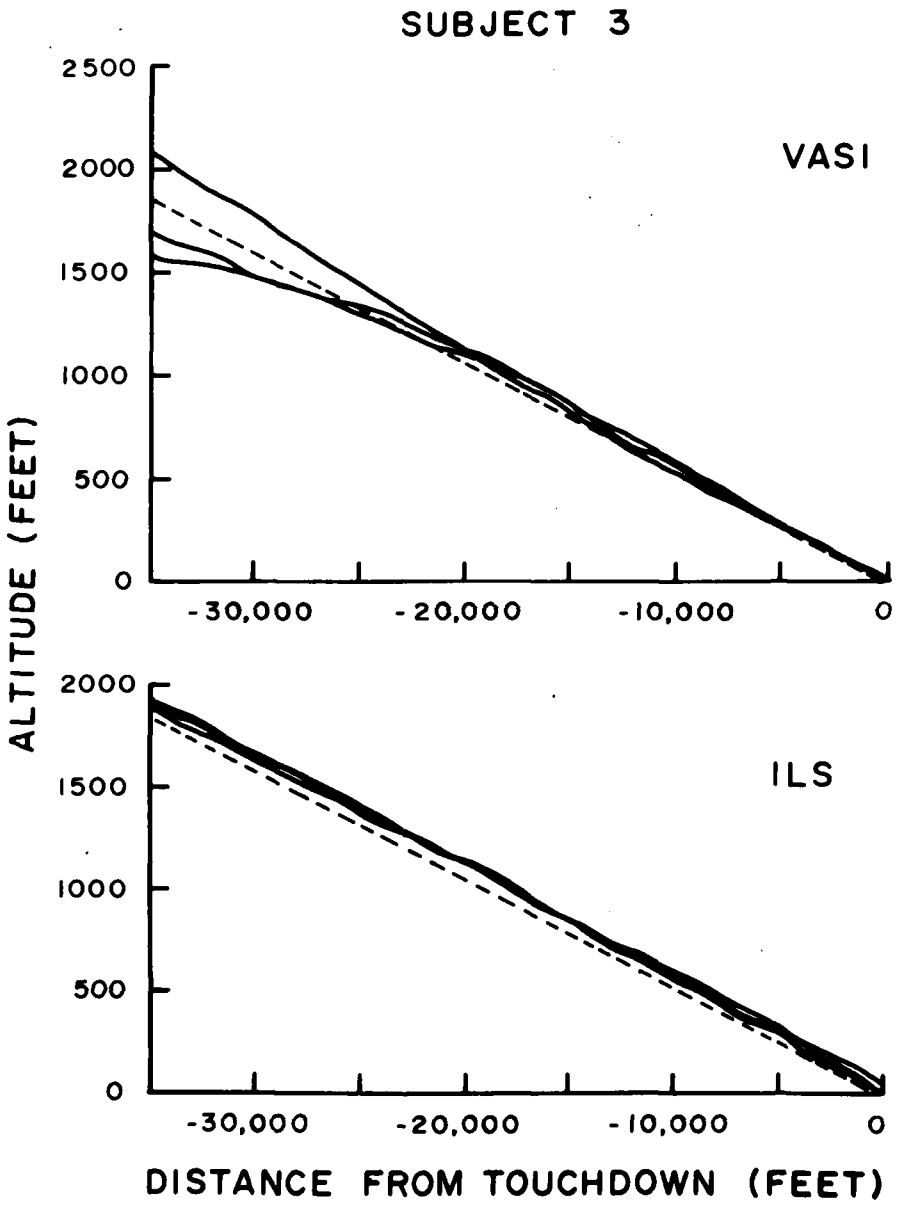

Figure 32. Approach path profiles for 2-bar VASI and ILS approaches for subject 3.

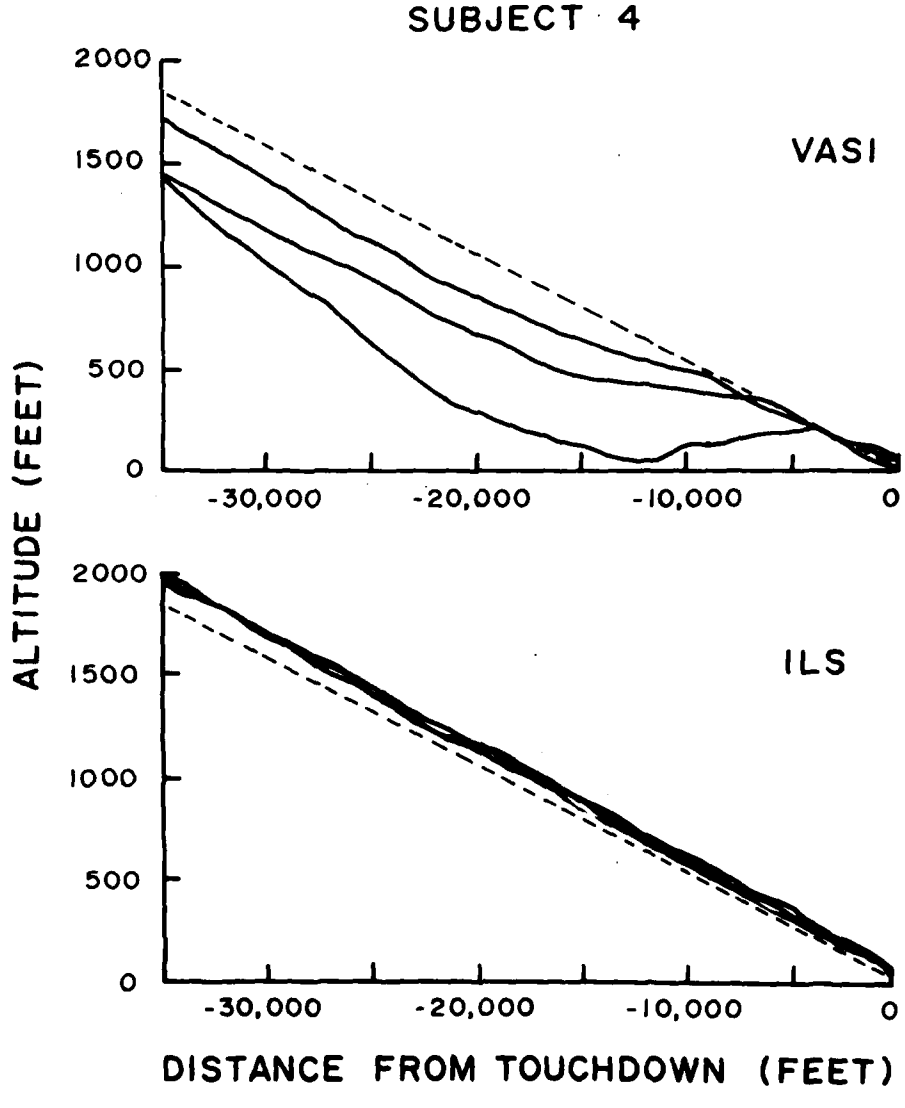

Figure 33. Approach path profiles for 2-bar VASI and ILS approaches for subject 4.

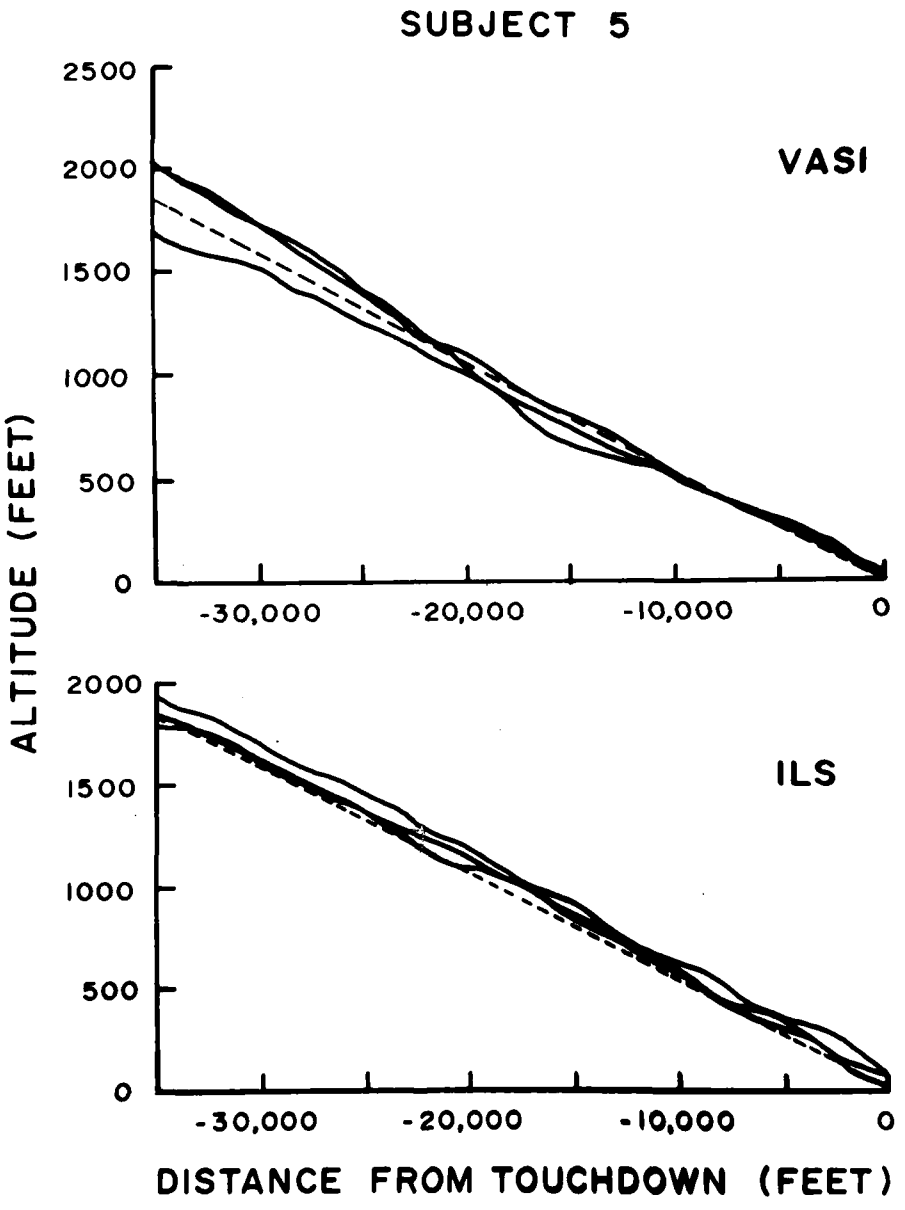

Figure 34. Approach path profiles for 2-bar VASI and ILS approaches for subject 5.

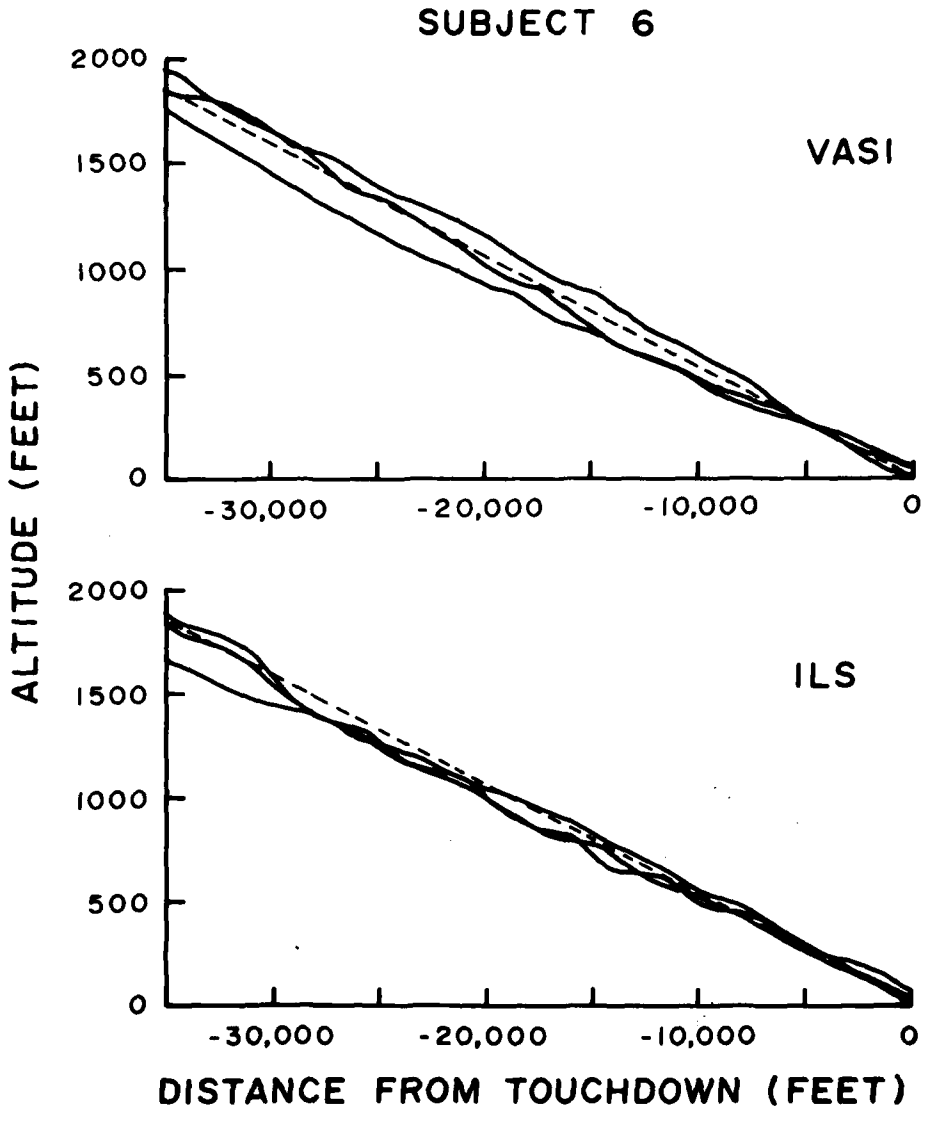

Figure 35. Approach path profiles for 2-bar VASI and ILS approaches for subject 6.

visual glidepath indicators during approaches in the simulated "black hole" situation where the only visible details of the ground plane are provided by runway lighting. This method is not seen as a substitute for operational evaluation of glidepath indicators, but as a possible preliminary way of examining strategies for analysis and defining important performance variables.